T-cell leukemia were described who had developed KS, from the Kyushu region and the southern island of Okinawa, but very few classic cases of KS were reported from other areas of Japan [Kamada et al., 1992]. After 1980, cases of AIDS-KS increased dramatically in Japan because of the rapid spread of AIDS. The introduction of highly active anti-retroviral therapy (HAART) reduced the number of KS cases in Western countries [Jones et al., 1999]. However, KS cases still increased in Japan after 2000 because of the dissemination of HIV infection within the homosexual male community. As well as AIDS-KS, other KSHV-associated diseases, such as AIDS-PEL and AIDS-MCD, also increased during the past 10 years in Japan [Katano et al., 1999a; Hasegawa et al., 2004; Abe et al., 2006]. Therefore, to prevent the spread of AIDS-KS, it is important to determine the clinicopathological features of KSHV-associated diseases in Japan. To date, reports describing the clinicopathological features of Japanese AIDS-KS have all involved only small sample sizes [Fujii et al., 1986; Kamada et al., 1992; Kondo et al., 2000; Yamada et al., 2000; Meng et al., 2001; Sato-Matsumura et al., 2001; Kamiyama et al., 2004; Minoda et al., 2006; Yoshii et al., 2006; Ueno et al., 2007].

The association of KSHV infection with KS pathogenesis has already been well investigated. A latency-associated nuclear antigen 1 (LANA-1) encoded by KSHV is detected in almost all KS cells, indicating that KS cells are infected with KSHV [Dupin et al., 1999; Katano et al., 1999b]. The genome of KSHV is a double-stranded linear DNA of about 170 kbp, flanked by GC-rich terminal repeats [Russo et al., 1996]. The *K1* gene in KSHV contains highly variable regions 1 and 2 (VR1, VR2) and phylogenetic analysis of the *K1* gene classified KSHV into genotypes A–F [Zong et al., 1997, 1999; Meng et al., 1999; Hayward and Zong, 2007]. These genotypes are differently distributed throughout the world: KSHV genotype A is predominant in North America, B in Africa, C in Eurasia and the Mediterranean, D in the Pacific islands, E in Brazilian Amerindians, and F in the Ugandan Bantu tribe [Zong et al., 1999; Biggar et al., 2000; Kajumbula et al., 2006]. Previous studies involving a small number of cases detected genotypes C and A in cases of KS, and genotype D in some cases of classic KS in Japan [Meng et al., 2001; Kamiyama et al., 2004]. However, it is unknown whether these genotypes are associated with any of the clinical features or pathogenesis of KS or other diseases.

In the present study, the clinicopathological features and genotypes of KSHV-associated diseases were investigated in 75 samples originating from all over Japan. The aim was to determine the characteristics of KSHV-associated diseases in Japan.

MATERIALS AND METHODS

Tissue Specimens

Studies using human tissue were performed with the approval of the Institutional Review Board of the National Institute of Infectious Diseases (Approval No. 158). Seventy-five cases of KSHV-associated disease were filed in the Department of Pathology, National Institute of Infectious Diseases, Japan, from 1995 to April 2009 as consultation cases. They include 68 KS cases, 5 PEL cases, and 5 MCD cases. Two MCD patients and a PEL patient had KS lesions. Frozen tissue samples were available for 21 of these cases. For some other cases, only formalin-fixed paraffin-embedded tissue sections were available. The samples were sent from all over Japan, from the northern island of Hokkaido to Okinawa, the southern island of Japan.

Histological Grading and Immunohistochemistry

Paraffin sections were hematoxylin and eosin stained and subjected to immunohistochemical staining to detect LANA-1, as described previously [Katano et al., 1999b]. Samples were categorized into three clinical stages of KS (patchy, plaque, or nodular stage) according to the clinical data and the histological findings.

Preparation of DNA

Total DNA was extracted from fresh-frozen clinical materials or formalin-fixed paraffin-embedded sections as described previously [Asahi-Ozaki et al., 2006]. For the isolation of DNA from formalin-fixed paraffin-embedded biopsies, three or four 5 μm-sections were placed into sterile eppendorf tubes, deparaffinized with xylene, digested with proteinase K, then extracted using the phenol/chloroform method. For fresh-frozen samples, DNA was extracted using the DNeasy Blood & Tissue kit according to the manufacturer's protocol (Qiagen GmbH, Hilden, Germany).

PCR Amplification and DNA Sequencing

A 160 bp fragment containing VR1 of the *K1* gene was amplified by PCR from DNA samples as described previously [Dilnur et al., 2001]. The primer set used was as follows: forward primer 5′-TTG CCA ATA TCC TGG TAT TGC-3′; reverse primer 5′-CAA GGT TTG TAA GAC AGG TTG-3′. PCR amplification was carried out at 94°C for 2 min (one cycle); 94°C for 1 min, 58°C for 1 min, and 72°C for 2 min (35 cycles); and 72°C for 5 min (one cycle) using the GeneAmp PCR System 9700 (Applied Biosystems, Foster City, CA). PCR products were purified using the QIAquick PCR purification kit (Qiagen), followed by direct sequencing with an ABI sequencer 3130 (Applied Biosystems) using a Big-Dye terminator ready reaction kit (Applied Biosystems) according to the manufacturer's instructions.

Phylogenetic Tree Analysis

Nucleotide sequences, excluding primer sequences, were multiple aligned with CLUSTAL W version 1.83 [Jeanmougin et al., 1998], and a phylogenetic tree was constructed using the neighbor-joining-plot method and Genetyx software (Genetyx, Tokyo, Japan). In addition

to our samples, 20 previously reported *K1* gene sequences were obtained from the GenBank database and used as reference sequences for comparison [Dilnur et al., 2001]. The genotypes of KSHV samples and the GenBank accession numbers of the reference strains are as follows: BCBL-R (genotype A, accession no. AF133038), BCBL-B (A, AF133039), 431KAP (B, AF133040), ASM72 (C, AF133041), BC2 (C, AF133042), TKS10 (D, AF133043), ZKS3 (D, AF133044), US3 (A, AF151688), Ug3 (A, AF151690), US6 (C, AF151686), Au1 (D, AF151687), Ug1 (B, AF151689), 78/48 (C, AF201851), 75/10T (A, AF201848), 80/56 (A, AF2-1853), KS-F (C, U93872), Tupi-1 (E, AF220292), Tupi-2 (AF220293), Wagu128 (E, AY940426), and BCBL-1 (A, U86667) [Meng et al., 1999; Zong et al., 1999; Lacoste et al., 2000; Kazanji et al., 2005]. BCBL-R was used as a consensus sequence.

GenBank Accession Numbers

GenBank accession numbers of Japanese KSHV sequences are AF278837 (J1), AF278842 (J2), AF278847–AF278849 (J3–J5), AF278850–AF278852 (J7–J9), AF278838 (J14), AF278839 (J16), AF278840 (J17), AF278841 (J19), AF278843 (J21), AF278844–AF278846 (J24–J26), and GQ848990–GQ849006 (J27–J43).

Statistical Analysis

Analysis of statistical significance was carried out using the Chi-squared test or Fisher's extract for bivariate tabular analysis and the Mann–Whitney test for comparison of two independent groups of sampled data.

RESULTS

Clinical and Pathological Characteristics of KS in Japan

Table I provides a summary of the clinical data. All of the cases were positive for LANA-1 by immunohistochemistry. The 68 pathological samples of KS were taken from various anatomical sites: the skin (84%), the gastrointestinal tract (7%), the lymph node (4%), the lungs (1%), the oral cavity (1%), and the conjunctive (1%) (Fig. 1A). Non-AIDS-KS cases were all presented in the skin. Among the 68 KS cases, 52 were AIDS-KS (76.4%) and 13 were non-AIDS-KS (19.1%). HIV-1 seropositive data were not available for three KS cases (4.4%). AIDS-KS cases were all from male patients with a mean age of 45.8 years (range: 23–82). By contrast, only six non-AIDS-KS cases were male (46%) and the proportion of female in non-AIDS-KS cases was high (54%). The mean age of non-AIDS-KS cases was 71.8 years (range: 52–87), which was statistically higher than that of AIDS-KS cases (Mann–Whitney test, $P < 0.01$). In addition, the mean age of non-AIDS-associated PEL cases was 97.5 years (range: 94–101), indicating occurrence of PEL in predominantly very elderly patients. Among the non-AIDS-KS cases, nine cases were regarded as classic KS and four cases were iatrogenic KS in immunosuppressed patients. Seven out of 13 non-AIDS-KS cases were in females, including 4 cases of iatrogenic KS. Histologically, the skin lesions of KS were categorized into stages: patchy (27%), plaque (36%), and nodular (34%) (Fig. 1B,C). Among the 13 non-AIDS-KS lesions, 6 lesions (46.2%) were at the plaque stage. However, AIDS-KS lesions represented all three stages, patchy, plaque, and nodular, almost equally. No histological difference was found between AIDS-KS and non-AIDS-KS.

Phylogenetic Tree Analysis of VR1 of the *K1* Gene From KSHV Genotypes

KSHV genotypes were determined in 33 cases based on the sequence of VR1 in the *K1* gene [Meng et al., 1999; Zong et al., 1999]. Thirty strains were obtained from KS samples, three from each of the PEL and MCD samples (Fig. 2A). Sixteen strains (J1–J5, J7–J9, J14, J16, J17, J19, J21, and J24–J26) have been described previously (14 KS, one PEL and one MCD case) [Meng et al., 2001]. Construction of a phylogenetic tree revealed that the Japanese cases were categorized into genotypes A, C, and D (Fig. 2B). Genotypes A and C were observed in the AIDS-KS subjects, whereas genotypes A, C, and D were observed in non-AIDS-KS subjects (Fig. 3A). Thus, genotype D was observed only in non-AIDS-KS subjects. All three cases of PEL, including one case of non-AIDS-PEL, were genotype C. Two genotype C and one genotype A sequences were detected in three cases of AIDS-MCD. Genotype A was detected more frequently

TABLE I. Summary of the Clinical Data of All Disease Cases Used in This Study

	n	Mean age	Age range	No. of males (%)	HIV(+)
KS	**68**	**50.7**	**23–87**	**61 (89.7%)**	**52/65 (80.0%)**
AIDS-KS	52	45.8	23–82	52 (100%)	—
Non-AIDS-KS	13	71.8	52–87	6 (46.1%)	—
Unknown	3	46.0	33–53	3 (100%)	—
PEL	**5***	**64.0**	**42–101**	**5* (100%)**	**3*/5 (60%)**
AIDS-PEL	3*	45.5	42–49	3* (100%)	—
Non-AIDS-PEL	2	97.5	94–101	2 (100%)	—
AIDS-MCD	**5****	**38.8**	**27–56**	**5** (100%)**	**5**/5 (100%)**
All	75	51.2	23–101	68 (90.7%)	57/72 (79.2%)

*Including one case having KS. **Including two cases having KS. Bold indicates large categories.

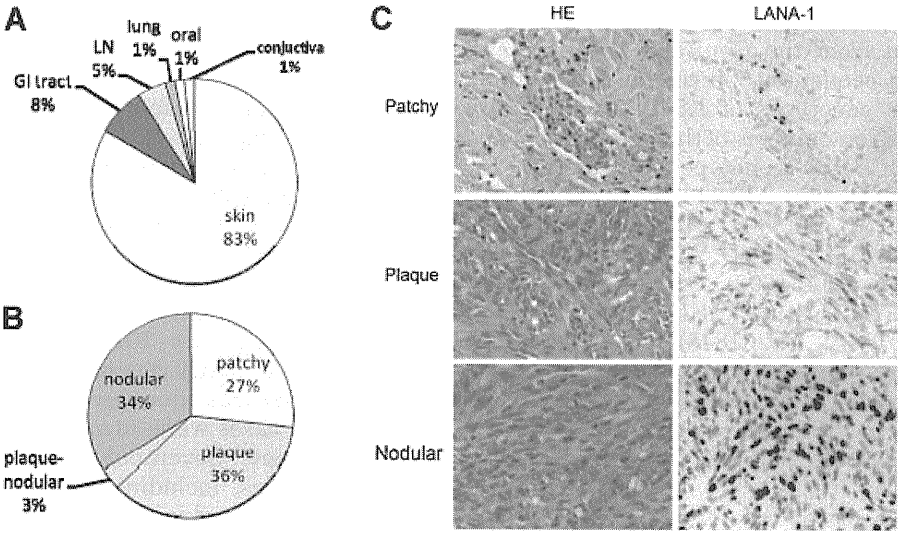

Fig. 1. Site and histology of Japanese Kaposi's sarcoma (KS) cases. Pie charts indicating (**A**) the site of KS and (**B**) the histological stage of KS in the skin, in the cases studied. GI: gastrointestinal, LN: lymph node. **C**: Hematoxylin and eosin (HE) staining (left) and latency-associated nuclear antigen 1 (LANA-1) immunohistochemistry (right) of patchy stage (upper), plaque (middle), and nodular stage (lower) of KS.

in AIDS-associated cases than non-AIDS-associated cases, but the difference was not statistically significant ($P = 0.28$, Chi-square test with Yate's correction) (Fig. 3B). Genotype C was common in both groups. The mean ages associated with genotypes A, C, and D were 48, 56, and 77, respectively. Genotype D was detected in more elderly patients than genotypes A and C ($P < 0.05$, Mann–Whitney test). These data indicated that genotype D was associated with non-AIDS-associated cases, not with AIDS-associated cases. The findings also suggest that genotype C is broadly distributed in Japan, and genotype A spreads among AIDS patients. There was no detectable histological difference among genotypes.

DISCUSSION

In this study, the clinicopathological features and genotypes of Japanese cases of KSHV-associated diseases were demonstrated. These data confirmed that non-AIDS-KSHV-associated diseases occurred predominantly in elderly patients. Genotype analyses suggested the broad distribution of genotype C, association of genotype D with non-AIDS-KS and spread of genotype A among AIDS patients in Japan.

There were few reports describing KS in Japan before 1986, and only 14 cases of classic KS were reported between 1917 and 1982 [Fujii et al., 1986]. A group in Okinawa reported six KS cases, including one adult T-cell leukemia-associated and two AIDS-associated cases in 1992 [Kamada et al., 1992]. After the discovery of KSHV in 1994, the association of KSHV infection in Japanese KS cases was proposed [Tachikawa et al., 1996]. Serological assays revealed that the seroprevalence of KSHV was 1.4% among the general population in Japan [Katano et al., 2000]. Almost all patients with AIDS-KS and non-AIDS-KS had serum antibody to KSHV, and 64% of Japanese AIDS patients, infected with HIV via sexual transmission were positive for anti-KSHV antibody [Katano et al., 2000]. KSHV was detected in all KS cases in Japan with positive immunohistochemical results for LANA-1 [Katano et al., 1999b]. Thus, the correlation between KSHV infection and KS pathogenesis has already been demonstrated in many Japanese cases. However, to date clinical information on Japanese KS cases was rarely reported [Fujii et al., 1986; Kamada et al., 1992; Kondo et al., 2000; Yamada et al., 2000; Kamiyama et al., 2004; Minoda et al., 2006; Yoshii et al., 2006; Ueno et al., 2007]. The difference in the mean age of patients affected by AIDS-KS and non-AIDS-KS was demonstrated in the present study. These results may reflect the population of origin for these patients. Several case studies reported that non-AIDS-KS in Japan is associated with immunosuppression, old age, or iatrogenic factors [Kondo et al., 2000; Yamada et al., 2000; Sato-Matsumura et al., 2001; Yoshii et al., 2006]. Regarding AIDS-KS, an epidemiological survey revealed that 70% of newly-HIV-infected individuals were infected via homosexual behavior (AIDS Surveillance Committee Japan, 2008). HAART decreased the incidence of KS in HIV-infected patients, but the increase of HIV-infection in homosexual men resulted in an increase of AIDS-KS cases in Japan. Although it is suggested that KSHV may be spread among homosexual men in Japan, further epidemiological studies on HIV-infected and uninfected males would be required to clarify the association of KSHV infection with the increase of KS in Japan.

KSHV genotypes are determined based on the sequence of VR1 in the *K1* gene sequence of KSHV [Meng et al., 1999; Zong et al., 1999]. Several variable regions were identified in the KSHV genome [Poole

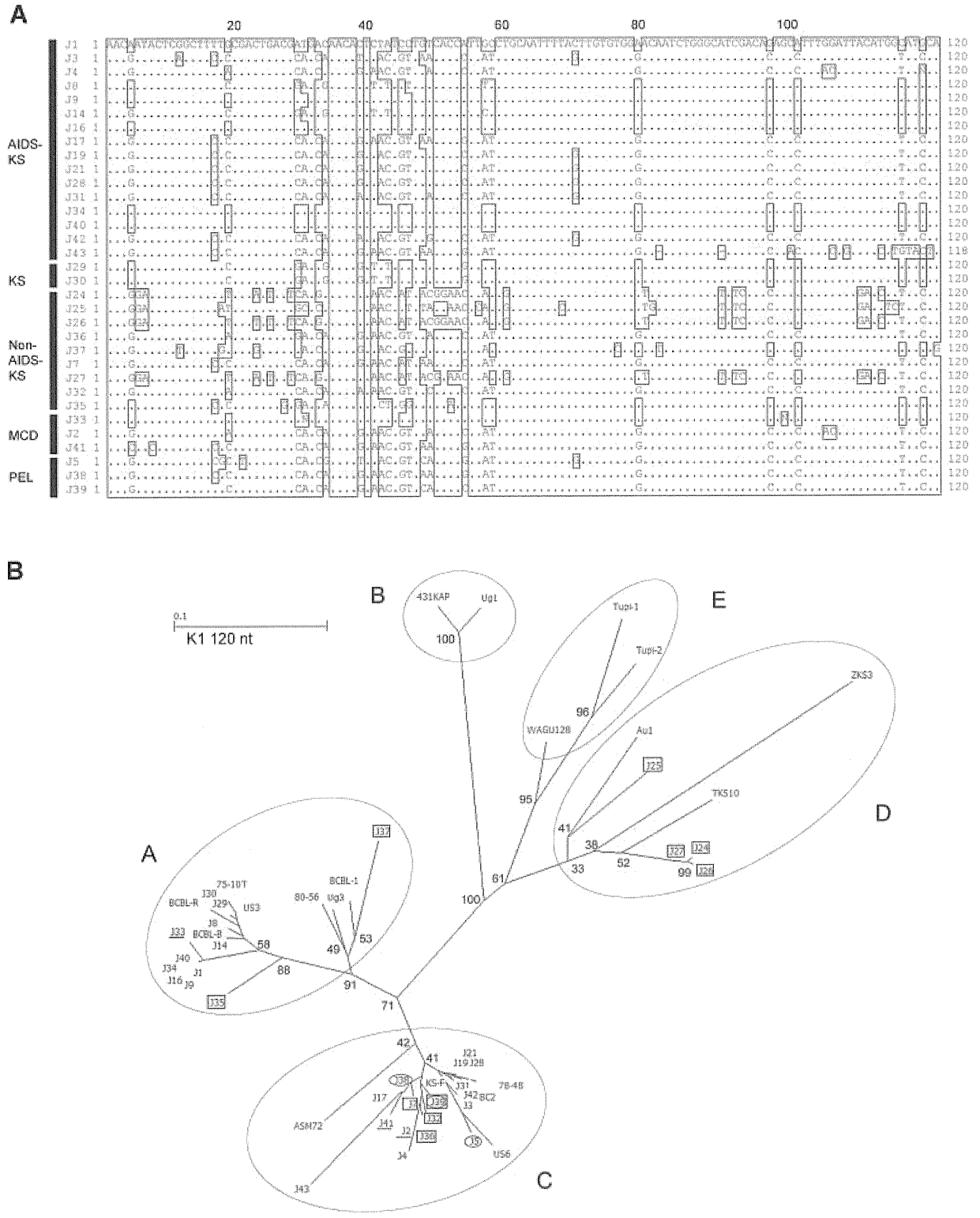

Fig. 2. K1 gene sequences in Japanese cases. **A**: Alignment of K1 gene sequences. One hundred twenty basepair fragments containing VR1 of the *K1* gene are shown. Case J33 had not only MCD, but also KS. HIV-1 seropositive data were not available for J29 and J30 cases. **B**: Radial unrooted phylogenetic tree generated by the NJ method on 120 bp segments of the *K1* gene. The numbers at some nodes (boot strap values) indicate frequencies of occurrence for 100 trees. Scale bar represents 0.1 substitutions per site. Genotypes A–E are indicated by circles. Japanese cases are indicated by J-numbers. J-numbers with boxes are non-AIDS cases of KS or PEL. J5 and J38 are AIDS-PEL cases (circled). J39 is a non-AIDS-PEL case (circled and boxed). J2, J33, and J41 are AIDS-MCD cases (underlined). All other sequences are included for reference. See text.

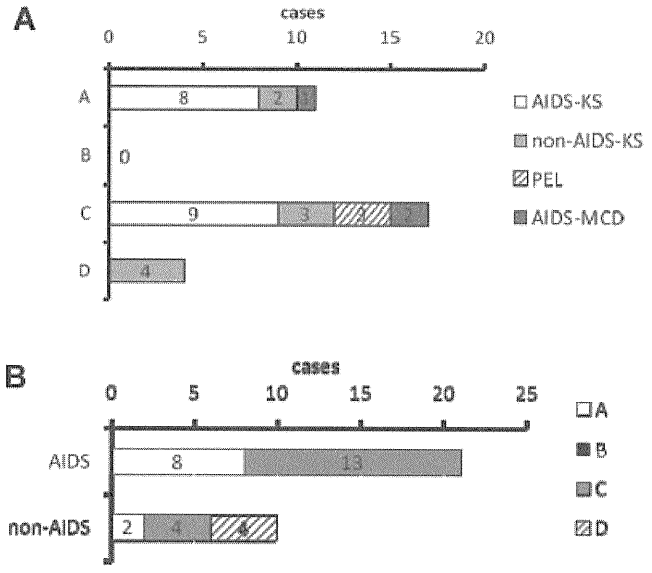

Fig. 3. Graphs indicating the association between: **A**: Kaposi's sarcoma-associated herpesvirus (KSHV) genotypes and diseases (each bar indicates the number of cases). **B**: Genotypes in AIDS-associated and non-AIDS-associated cases.

et al., 1999]. However, since frequent variations were detected in the *K1* gene among strains, the *K1* gene was well investigated and used as a standard for genotype determination [Meng et al., 1999; Zong et al., 1999; Hayward and Zong, 2007]. Genotypes A and C of KSHV are broadly distributed throughout the world. A previous study had already shown that genotype C was predominant not only in Japan, but also in Asian countries, such as Taiwan, Korea, and China [Zong et al., 2002]. Genotype C was detected in Uygur people in Xinjiang, west of China, that was located at the middle point of the Silk Road from Rome to Xian, China [Dilnur et al., 2001]. The virus may therefore have been transmitted via the migration of people from Europe, and the genotype C virus spread in Asian countries. Genotype D, found in the Oceania region, had already been detected in three cases of non-AIDS-KS in Japan in a previous study [Meng et al., 2001]. One additional case of genotype D was found in a non-AIDS-KS case in the present study, supporting the association of genotype D with non-AIDS-KS. Genotype A was detected in both AIDS-KS and non-AIDS-KS cases in the present study. To date, there has been no report of genotype A in non-AIDS-KS cases in Japan. Genotype A was more frequently found in AIDS-KS cases, suggesting that genotype A came from the USA via homosexual activity. However, detection of genotype A in non-AIDS-KS cases at a low rate suggests that genotype A is also a common virus in the general population in Japan, along with genotype C.

PEL and MCD are very rare diseases associated with KSHV infection. A previous study demonstrated that only AIDS-MCD is associated with KSHV infection, not non-AIDS-MCD in Japan [Suda et al., 2001]. All three cases of PEL investigated in this study were genotype C virus, while two genotype C and one genotype A were detected in three cases of MCD. There was no correlation between KSHV genotype and disease, suggesting that any genotype in Japan may induce any type of KSHV-associated disease. Considering 1.4% of KSHV seroprevalence in the general population in Japan, there may be many KSHV-infected individuals without symptoms [Katano et al., 2000]. Although genotype analysis suggests transmission routes of the virus from other countries, further studies using a large number of KSHV-infected patients are needed to clarify the route of KSHV infection among individuals.

REFERENCES

Abe Y, Matsubara D, Gatanaga H, Oka S, Kimura S, Sasao Y, Saitoh K, Fujii T, Sato Y, Sata T, Katano H. 2006. Distinct expression of Kaposi's sarcoma-associated herpesvirus-encoded proteins in Kaposi's sarcoma and multicentric Castleman's disease. Pathol Int 56:617–624.

Antman K, Chang Y. 2000. Kaposi's sarcoma. N Engl J Med 342:1027–1038.

Asahi-Ozaki Y, Sato Y, Kanno T, Sata T, Katano H. 2006. Quantitative analysis of Kaposi sarcoma-associated herpesvirus (KSHV) in KSHV-associated diseases. J Infect Dis 193:773–782.

Biggar RJ, Whitby D, Marshall V, Linhares AC, Black F. 2000. Human herpesvirus 8 in Brazilian Amerindians: A hyperendemic population with a new subtype. J Infect Dis 181:1562–1568.

Chang Y, Cesarman E, Pessin MS, Lee F, Culpepper J, Knowles DM, Moore PS. 1994. Identification of herpesvirus-like DNA sequences in AIDS-associated Kaposi's sarcoma. Science 266:1865–1869.

Dilnur P, Katano H, Wang ZH, Kudo M, Osakabe Y, Sata T, Ebihara Y. 2001. Classic type of Kaposi's sarcoma and human herpesvirus 8 infection in Xinjiang, China. Pathol Int 51:845–852.

Dupin N, Fisher C, Kellam P, Ariad S, Tulliez M, Franck N, van ME, Salmon D, Gorin I, Escande JP, Weiss RA, Alitalo K, Boshoff C. 1999. Distribution of human herpesvirus-8 latently infected cells in Kaposi's sarcoma, multicentric Castleman's disease, and primary effusion lymphoma. Proc Natl Acad Sci USA 96:4546–4551.

Fujii Y, Takayasu S, Yokoyama S, Eizuru Y, Minamishima Y, Enjoji M. 1986. Kaposi's sarcoma in a Korean living in Japan. Review of cases reported in Japanese literature. J Am Acad Dermatol 15:76–82.

Hasegawa H, Katano H, Tanno M, Masuo S, Ae T, Sato Y, Takahashi H, Iwasaki T, Kurata T, Sata T. 2004. BCL-6-positive human herpesvirus 8-associated solid lymphoma arising from liver and spleen as multiple nodular lesions. Leuk Lymphoma 45:2169–2172.

Hayward GS, Zong JC. 2007. Modern evolutionary history of the human KSHV genome. Curr Top Microbiol Immunol 312:1–42.

Jeanmougin F, Thompson JD, Gouy M, Higgins DG, Gibson TJ. 1998. Multiple sequence alignment with Clustal X. Trends Biochem Sci 23:403–405.

Jones JL, Hanson DL, Dworkin MS, Ward JW, Jaffe HW. 1999. Effect of antiretroviral therapy on recent trends in selected cancers among HIV-infected persons. Adult/Adolescent Spectrum of HIV Disease Project Group. J Acquir Immune Defic Syndr 21:S11–S17.

Kajumbula H, Wallace RG, Zong JC, Hokello J, Sussman N, Simms S, Rockwell RF, Pozos R, Hayward GS, Boto W. 2006. Ugandan Kaposi's sarcoma-associated herpesvirus phylogeny: Evidence for cross-ethnic transmission of viral subtypes. Intervirology 49:133–143.

Kamada Y, Iwamasa T, Miyazato M, Sunagawa K, Kunishima N. 1992. Kaposi sarcoma in Okinawa. Cancer 70:861–868.

Kamiyama K, Kinjo T, Chinen K, Iwamasa T, Uezato H, Miyagi JI, Mori N, Yamane N. 2004. Human herpesvirus 8 (HHV8) sequence variations in HHV8 related tumours in Okinawa, a subtropical island in southern Japan. J Clin Pathol 57:529–535.

Kaposi M. 1872. Idiopatiches multiples pigment sarcom der Haut. Arch Dermatol Syphil 4:265–272.

Katano H, Hoshino Y, Morishita Y, Nakamura T, Satoh H, Iwamoto A, Herndier B, Mori S. 1999a. Establishing and characterizing a CD30-positive cell line harboring HHV-8 from a primary effusion lymphoma. J Med Virol 58:394–401.

Katano H, Sato Y, Kurata T, Mori S, Sata T. 1999b. High expression of HHV-8-encoded ORF73 protein in spindle-shaped cells of Kaposi's sarcoma. Am J Pathol 155:47–52.

Katano H, Iwasaki T, Baba N, Terai M, Mori S, Iwamoto A, Kurata T, Sata T. 2000. Identification of antigenic proteins encoded by human herpesvirus 8 and seroprevalence in the general population and among patients with and without Kaposi's sarcoma. J Virol 74: 3478–3485.

Kazanji M, Dussart P, Duprez R, Tortevoye P, Pouliquen JF, Vandekerkhove J, Couppie P, Morvan J, Talarmin A, Gessain A. 2005. Serological and molecular evidence that human herpesvirus 8 is endemic among Amerindians in French Guiana. J Infect Dis 192: 1525–1529.

Kondo Y, Izumi T, Yanagawa T, Kanda H, Katano H, Sata T. 2000. Spontaneously regressed Kaposi's sarcoma and human herpesvirus 8 infection in a human immunodeficiency virus-negative patient. Pathol Int 50:340–346.

Lacoste V, Kadyrova E, Chistiakova I, Gurtsevitch V, Judde JG, Gessain A. 2000. Molecular characterization of Kaposi's sarcoma-associated herpesvirus/human herpesvirus-8 strains from Russia. J Gen Virol 81:1217–1222.

Meng YX, Spira TJ, Bhat GJ, Birch CJ, Druce JD, Edlin BR, Edwards R, Gunthel C, Newton R, Stamey FR, Wood C, Pellett PE. 1999. Individuals from North America, Australasia, and Africa are infected with four different genotypes of human herpesvirus 8. Virology 261:106–119.

Meng YX, Sata T, Stamey FR, Voevodin A, Katano H, Koizumi H, Deleon M, De Cristofano MA, Galimberti R, Pellett PE. 2001. Molecular characterization of strains of Human herpesvirus 8 from Japan, Argentina and Kuwait. J Gen Virol 82:499–506.

Minoda H, Usui N, Sata T, Katano H, Serizawa H, Okada S. 2006. Human Herpesvirus-8 in Kaposi's Sarcoma of the Conjunctiva in a Patient with AIDS. Jpn J Ophthalmol 50:7–11.

Moore PS, Chang Y. 2001. Kaposi's sarcoma-associated herpesvirus. In: Knipe DM, Howley PM, editors. Fields Virology 4th ed. Philadelphia: Lippincott Williams & Wilkins, pp 2803–2834.

Poole LJ, Zong JC, Ciufo DM, Alcendor DJ, Cannon JS, Ambinder R, Orenstein JM, Reitz MS, Hayward GS. 1999. Comparison of genetic variability at multiple loci across the genomes of the major subtypes of Kaposi's sarcoma-associated herpesvirus reveals evidence for recombination and for two distinct types of open reading frame K15 alleles at the right-hand end. J Virol 73:6646–6660.

Russo JJ, Bohenzky RA, Chien MC, Chen J, Yan M, Maddalena D, Parry JP, Peruzzi D, Edelman IS, Chang Y, Moore PS. 1996. Nucleotide sequence of the Kaposi sarcoma-associated herpesvirus (HHV8). Proc Natl Acad Sci USA 93:14862–14867.

Sato-Matsumura KC, Matsumura T, Nabeshima M, Katano H, Sata T, Koizumi H. 2001. Serological and immunohistochemical detection of human herpesvirus 8 in Kaposi's sarcoma after immunosuppressive therapy for bullous pemphigoid. Br J Dermatol 145:633–637.

Suda T, Katano H, Delsol G, Kakiuchi C, Nakamura T, Shiota M, Sata T, Higashihara M, Mori S. 2001. HHV-8 infection status of AIDS-unrelated and AIDS-associated multicentric Castleman's disease. Pathol Int 51:671–679.

Tachikawa N, Goto M, Gatanaga H, Katano H, Oka S, Wakabayashi T, Mori S, Iwamoto A. 1996. Herpesvirus-like DNA sequences in Japanese patients with AIDS-related Kaposi's sarcoma. J Infect Chemother 1:190–192.

Ueno T, Mitsuishi T, Kimura Y, Kato T, Hasegawa H, Katano H, Sata T, Kurane S, Kawana S. 2007. Immune reconstitution inflammatory syndrome associated with Kaposi's sarcoma: Successful treatment with interferon-alpha. Eur J Dermatol 17:539–540.

Yamada Y, Funasaka Y, Nishioka E, Okuno T, Ichihashi M. 2000. A case of classic Kaposi's sarcoma in a Japanese man: Detection of human herpes virus 8 (HHV-8) infection by means of polymerase chain reaction and immunofluorescence assay. J Dermatol 27:391–396.

Yoshii N, Kanekura T, Eizuru Y, Setoyama M, Kanzaki T, Yamanishi K. 2006. Transcripts of the human herpesvirus 8 genome in skin lesions and peripheral blood mononuclear cells of a patient with classic Kaposi's sarcoma. Clin Exp Dermatol 31:125–127.

Zong JC, Metroka C, Reitz MS, Nicholas J, Hayward GS. 1997. Strain variability among Kaposi sarcoma-associated herpesvirus (human herpesvirus 8) genomes: Evidence that a large cohort of United States AIDS patients may have been infected by a single common isolate. J Virol 71:2505–2511.

Zong JC, Ciufo DM, Alcendor DJ, Wan X, Nicholas J, Browning PJ, Rady PL, Tyring SK, Orenstein JM, Rabkin CS, Su IJ, Powell KF, Croxson M, Foreman KE, Nickoloff BJ, Alkan S, Hayward GS. 1999. High-level variability in the ORF-K1 membrane protein gene at the left end of the Kaposi's sarcoma-associated herpesvirus genome defines four major virus subtypes and multiple variants or clades in different human populations. J Virol 73:4156–4170.

Zong J, Ciufo DM, Viscidi R, Alagiozoglou L, Tyring S, Rady P, Orenstein J, Boto W, Kalumbuja H, Romano N, Melbye M, Kang GH, Boshoff C, Hayward GS. 2002. Genotypic analysis at multiple loci across Kaposi's sarcoma herpesvirus (KSHV) DNA molecules: Clustering patterns, novel variants and chimerism. J Clin Virol 23:119–148.

508

臨床研究の進歩　合併症の治療と対策

免疫再構築症候群への対応

古西　満[1]　宇野健司[1]　善本英一郎[2]

Management of immune reconstitution inflammatory syndrome

[1]Mitsuru Konishi, [1]Kenji Uno, [2]Eiichiro Yoshimoto
[1]Center for Infectious Diseases, Nara Medical University
[2]Division of Infection Control, Nara Kohsei-kai Hospital

Abstract

While antiretroviral therapy (ART) in HIV-infected patients results in dramatic reductions in HIV viral load and subsequent improvements in CD4 cell count, part of patients experience clinical deterioration as a direct consequence of rapid and dysregulated restoration of antigen-specific immune responses. This is termed "immune reconstitution inflammatory syndrome (IRIS)." Because there is no single agreed upon definition for IRIS, the diagnosis of IRIS is clinical. Several studies have demonstrated that lower CD4 cell count and higher viral load at the initiation of ART increase the risk of developing IRIS. Management of IRIS consists of appropriate treatment for the diseases of IRIS, control of the excessive inflammation (NSAIDs or corticosteroids), and interrupting ART.

Key words: immune reconstitution inflammatory syndrome, antiretroviral therapy, risk factor, management

はじめに

有効な抗HIV治療を開始すると，1-2週間でウイルス量は90％以上減少し，その後8-12週間は減少を続けて定常状態となる．このウイルス量の減少とは逆に単球，マクロファージ，NK細胞の機能は回復し，CD4陽性細胞数も増加してくる．

この時期には，既に治療した感染症の再発やそれまで臨床的に明らかでなかった感染症の発症などを認めることがある．これは，免疫系の再構築が体内に存在する病原体などの抗原に対する免疫応答を誘導して起こると考えられ，免疫再構築症候群(immune reconstitution inflammatory syndrome: IRIS)と呼ばれている．

しかし，IRISに関する十分なエビデンスはまだ集積されていないため，本稿では，現時点で考えられているIRISの臨床的概念，発症リスク，対処法などについて解説する．

1. IRISの診断と臨床分類

IRISの診断基準はいまだに確立していないが，Shelburneら[1]の提案はIRISの概念を理解するうえで有用である(**表1**)．現時点では高度の免疫不全があるHIV感染者に新規の抗HIV治療を開始，もしくは効果不十分な治療を有効な抗

[1]奈良県立医科大学感染症センター　[2]奈良厚生会病院 感染制御室

0047-1852/10/¥40/頁/JCOPY

表1 Shelburneらによる免疫再構築症候群(IRIS)の診断基準(文献[1]より引用)

1) HIV(+)
2) HAARTを行っている
   ・HIV-RNA量の減少
   ・CD4陽性細胞の増加(HIV-RNA量の減少より遅れてもよい)
3) 炎症過程に矛盾しない臨床症候がある
4) 以下の臨床経過を除外
   ・既に診断された日和見感染症で予測される経過
   ・新たに診断される日和見感染症として予測される経過
   ・薬剤の副作用

表2 免疫再構築症候群(IRIS)の臨床分類(文献[2]より改変)

分類	対象となる抗原	実例
感染症(顕在化型)	増殖している病原体	クリプトコッカス髄膜炎の顕在化
感染症(矛盾悪化型)	死滅している病原体	治療後のニューモシスチス肺炎の悪化
自己免疫	宿主の抗原	Graves病
悪性腫瘍	腫瘍/発癌病原体	Kaposi肉腫
その他の炎症	様々	サルコイドーシス

HIV治療に変更した後，数カ月以内に日和見感染症などの疾患が発症，再発，再増悪した場合にはIRISとして対応することが妥当であると考えている．診断する際には，少なくとも開始した抗HIV治療が有効であることを確認し(血中HIV-RNA量の低下)，使用中の抗HIV薬などの副作用を除外する必要がある．

IRISの多くは日和見感染症の病原体が抗原となっているが，宿主の抗原(自己免疫)や腫瘍/発癌病原体の抗原(悪性腫瘍)などに免疫応答を生じることもある．感染症のIRISには，診断がされていない未治療の感染症が抗HIV治療後に顕在化する場合(顕在化型)と，治療によって改善・治癒していた感染症が抗HIV治療後に再増悪・再発する場合(矛盾悪化型)とがある(**表2**)[2]．

2. IRISの疫学

確立した診断基準がなく，大規模な疫学調査が行われていないため，正確なIRISの発症率はわかっていない．これまでの比較的規模の大きな後向き調査では，抗HIV治療を受けた患者の17-25％に発症すると報告されている．南アフリカにおけるナイーブ症例423例の前向き調査では44例(10.4％)にIRISを発症し，発症率は100人年あたり25.1例であったと報告している[3]．我が国の調査では，抗HIV治療を受けた2,018例中176例(8.7％)にIRISを発症していたが，施設別の発症率は2.0-15.4％と差異があり[4]，IRISの発症率には症例背景や各施設の治療方針などの違いが影響すると考えられる．

IRISとして発症する疾患も各報告によって様々である．例えば，前述の南アフリカでの調査では結核症，帯状疱疹，単純ヘルペス，クリプトコッカス髄膜炎などの順に多く認められている[3]．ところが，我が国の調査では帯状疱疹，非結核性抗酸菌症，サイトメガロウイルス感染症，ニューモシスチス肺炎，結核症，Kaposi肉腫，進行性多巣性白質脳症などの順となっている[4]．

3. IRIS発症の危険因子

IRIS発症の危険因子についても様々な報告があり，いまだに明確な結論は得られていない．

これまでに抗HIV治療開始時のCD4陽性細胞数低値やHIV-RNA量高値が危険因子である

ことは指摘されている．著者らも抗HIV治療開始時にCD4陽性細胞数50/μL未満の症例ではodds比が5.78(95％CI: 2.38-14.08, p<0.001), HIV-RNA量10万コピー/mL以上の症例ではodds比が3.10(95％CI: 1.38-6.93, p<0.05)となることを報告している[5]．

また，抗HIV治療によってHIV-RNA量が急速に低下することが危険因子の一つであるとの指摘もみられる．2008年発売されたインテグラーゼ阻害薬raltegravir(RAL)は強力な抗HIV効果を示し，非核酸系逆転写酵素阻害薬efavirenz(EFV)を用いた抗HIV治療に比べ有意に早くHIV-RNA量50コピー/mL未満を達成している．ところが，IRISの発症率はRALを用いた抗HIV治療が6％，EFVを用いた抗HIV治療が4％と有意差はなく[6]，HIV-RNA量の急速な低下とIRIS発症には関連がない可能性も考えられる．

Manabeら[7]は，ritonavir(RTV)を併用するプロテアーゼ阻害薬治療(boosted PI)がIRIS発症に関連すると報告している．PIは，*in vitro*でT細胞の増殖やアポトーシスに影響することやマクロファージからの炎症性サイトカイン産生を誘導することが認められる．そのため，PIはHIV増殖抑制とは別の機序でIRIS発症に関与する可能性が推測されている．

4. IRISへの対処法

IRISを回避するための方法やIRISを発症したときの対応もいまだに確立していない．したがって，以下にはこれまでの経験から考えられる対処法について述べる(表3)．

a. 抗HIV治療開始前

IRISの疾患は事前に把握しにくいこともあるので，抗HIV治療開始前には日和見合併症の有無を注意深く評価する．免疫不全が進行した症例，特にCD4陽性細胞数が50/μL未満の症例では，眼底検査，胸部X線写真，血液検査(β-Dグルカン，クリプトコッカス抗原，サイトメガロウイルス抗原など)，可能ならば脳MRIなどをスクリーニングしておく．

また，CD4陽性細胞数50/μL未満の症例には非結核性抗酸菌症，200/μL未満の症例にはニューモシスチス肺炎に対する予防を開始する．照屋ら[8]は，予防の徹底によって非結核性抗酸菌症のIRIS発症が減少したことを報告している．

表3 免疫再構築症候群(IRIS)への対処法

抗HIV治療前
1. 顕在化していない日和見合併症の評価
   ・気がついていない合併症がないかを確認
   (例えば，眼底検査，CMV抗原検査など)
2. 対象となる日和見感染症の予防
   ・ニューモシスチス肺炎，MAC感染症など
3. 発症した日和見感染症の十分な治療

IRIS発症時
1. IRISの疾患に対する治療
2. 過剰な炎症のコントロール
   ・NSAIDs
   ・副腎皮質ステロイド薬
3. 最終手段として抗HIV治療の中止

日和見合併症の治療後いつから抗HIV治療を開始するかについても結論は出ていない．IRISを回避するには体内の病原体抗原量を十分に減らしてから抗HIV治療を開始することが望ましいが，抗HIV治療開始を遅らせることでほかの日和見合併症を発症するリスクがあり，悩ましい問題である．我が国では日和見感染症の治療を行ってから抗HIV治療を開始する傾向があるが，欧米では早期に抗HIV治療を導入することを推奨する傾向にある．

b. IRIS発症時

IRISを発症しても有効な抗HIV治療をできるかぎり継続することが基本である．

IRISへの対応には，疾患自体の治療と過剰な炎症のコントロールとがある．疾患が感染症のときは病原体の増殖がなければ，抗微生物薬を投与しないという考え方もある．しかし，実際に病原体の増殖がないことを証明するのは難しく，IRISが軽症である場合を除けば抗微生物薬の開始・追加・変更が必要であると考える．炎症をコントロールする方法には，NSAIDsや副腎皮質ステロイド薬の投与がある．副腎皮質ステロイド薬は，臓器障害が重篤，または生命の危機がある場合で他の方法が無効なときに考慮

する．一般にプレドニゾロン1mg/kg/日（最大投与量60-80mg/日）で開始し，週から月単位で減量することが多い．

また，IRISのために抗HIV治療を中止することもあるが，その基準も決まっていない．現時点では，抗HIV治療の継続が生命を脅かす場合や副腎皮質ステロイド薬が無効な場合などに抗HIV治療の中止を考慮している．

おわりに

IRISは患者の治療計画を妨げることから，発症を予防できることが望ましい．しかし，いまだに確実な診断ができないためにIRISの研究はなかなか進展しない状況にある．今後の研究成果によって効果的，かつ安全性の高い抗HIV治療が可能になることが望まれる．

文　献

1) Shelburne SA, et al: Immune reconstitution inflammatory syndrome: more answers, more questions. J Antimicrob Chemother **57**: 167-170, 2006.
2) Dhasmana DJ, et al: Immune reconstitution inflammatory syndrome in HIV-infected patients receiving antiretroviral therapy: Pathogenesis, clinical manifestations and management. Drugs **68**: 191-208, 2008.
3) Murdoch DM, et al: Incidence and risk factors for the immune reconstitution inflammatory syndrome in HIV patients in South Africa: a prospective study. AIDS **22**: 601-610, 2008.
4) 古西　満ほか：免疫再構築症候群の発症状況調査．厚生労働科学研究エイズ対策事業「HAART時代の日和見合併症に関する研究」平成15年度報告書，p82-87，2004.
5) 古西　満ほか：免疫再構築症候群に関する調査および情報提供．厚生労働科学研究エイズ対策事業「重篤な日和見感染症と最適治療に関する研究」平成20年度報告書，p53-60，2009.
6) Lennox JL, et al: Safety and efficacy of raltegravir-based versus efavirenz-based combination therapy in treatment-naïve patients with HIV-1 infection: a multicentre, double-blind randomized controlled trial. Lancet **374**: 796-806, 2009.
7) Manabe YC, et al: Immune reconstitution inflammatory syndrome: Risk factors and treatment implications. J Acquir Immune Defic Syndr **46**: 456-462, 2007.
8) 照屋勝治ほか：HIV感染者における免疫再構築症候群（サイトメガロウイルス網膜炎）発症予防に関する研究．厚生労働科学研究エイズ対策事業「重篤な日和見感染症と最適治療に関する研究」平成19年度報告書，p34-38，2008.

JLB

Article

HIV-1 Vpr induces TLR4/MyD88-mediated IL-6 production and reactivates viral production from latency

Shigeki Hoshino,[*,†] Mitsuru Konishi,[‡] Masako Mori,[§] Mari Shimura,[*] Chiaki Nishitani,[‖] Yoshio Kuroki,[‖] Yoshio Koyanagi,[¶] Shigeyuki Kano,*[,†] Hiroyuki Itabe,[**] and Yukihito Ishizaka*[,1]*

[*]Research Institute, International Medical Center of Japan, Tokyo, Japan; [†]Graduate School of Comprehensive Human Sciences, University of Tsukuba, Tsukuba, Japan; [‡]Center for Infectious Diseases, Nara Medical University, Nara, Japan; [§]Laboratory of Glyco-Organic Chemistry, The Noguchi Institute, Tokyo, Japan; [‖]Department of Biochemistry, Sapporo Medical University School of Medicine, Hokkaido, Japan; [¶]Laboratory of Viral Pathogenesis, Institute for Virus Research, Kyoto University, Kyoto, Japan; and [**]Department of Biological Chemistry, School of Pharmacy, Showa University, Tokyo, Japan

RECEIVED AUGUST 11, 2009; REVISED DECEMBER 10, 2009; ACCEPTED JANUARY 21, 2010. DOI: 10.1189/jlb.0809547

ABSTRACT

Vpr, a HIV-1 accessory protein, was believed to be present in the plasma of HIV-1-positive patients, and our previous work demonstrated the presence of plasma Vpr in 20 out of 52 patients. Interestingly, our data revealed that patients' viral titer was correlated with the level of Vpr detected in their plasma. Here, we first show that rVpr, when incubated with human monocytes or MDMs, caused viral production from latently infected cells, and IL-6 was identified as a responsible factor. The induction of IL-6 by rVpr was dependent on signaling through TLR4 and its adaptor molecule, MyD88. We next provide evidence that rVpr induced the formation of OxPC and that a mAb against OxPC blocked rVpr-induced IL-6 production with the concomitant attenuation of MAPK activation. Moreover, the addition of NAC, a scavenger of ROS, abrogated the rVpr-induced formation of OxPC, the phosphorylation of C/EBP-β, a substrate of MAPK, and IL-6 production. As rIL-6 reactivated viral replication in latently infected cells, our data indicate that rVpr-induced oxidative stress triggers cell-based innate immune responses and reactivates viral production in latently infected cells via IL-6 production. Our results suggest that Vpr should be monitored based on the viral titer, and they provide the rationale for the development of novel, anti-AIDS therapeutics targeting Vpr. *J. Leukoc. Biol.* 87: 1133–1143; 2010.

Introduction

The complete eradication of HIV-1 from infected patients remains problematic, although the use of HAART has improved the prognosis of patients who are HIV-positive [1]. A major obstacle to total viral eradication is the persistence of viral reservoirs [2, 3] from which reactivation of viral production can be initiated in response to exogenous factors such as cytokines [4, 5], ultraviolet irradiation [6], and DNA damage [6]. As infected macrophages are a major component of viral reservoirs [7–9], clarifying the mechanism of the reactivation of viral replication in latently infected macrophages is important.

Vpr, an accessory gene encoded by the HIV-1 genome, has at least two activities that up-regulate viral replication in macrophages. First, *Vpr* is required for the primary viral infection of resting macrophages and was shown to contribute to the translocation of the preintegration complex from the cytoplasm to the nucleus [10]. Second, Vpr is present in the plasma of infected patients, and exogenously added Vpr can induce viral reproduction in latently infected cells [11, 12]. Recently, we analyzed the level of Vpr in the plasma of HIV-1-positive individuals and detected the protein in 20 out of 52 patients examined [13]. Our data also revealed that the detection of Vpr was coupled with a high copy number of HIV-1 RNA [13], implying that Vpr functions as a positive regulator of viral replication in vivo.

In addition to viral production, mitochondrial dysfunction is a particularly important property of Vpr in AIDS pathogenesis

Abbreviations: ACTB=β-actin, ALLN=N-acetyl-L-leucyl-L-leucyl-L-norleucinal, ANT=adenine nucleotide translocator, CBB=Coomassie brilliant blue, CM=conditioned medium, ΔC12=C-terminal-most 12 aa, H5N1=avian influenza virus, HAART=highly active antiretroviral therapy, HIF-1=hypoxia-inducible factor-1, IKK=IκB kinase, LAL=Limulus amebocyte lysate, LSC=laser-scanning cytometer, MDM=monocyte-derived macrophage, MMP=mitochondrial membrane potential, NAC=N-acetyl-cysteine, OxPC=oxidized phosphatidylcholine(s), PFA=paraformaldehyde, qPCR=quantitative PCR, RIPA=radioimmunoprecipitation assay, ROS= reactive oxygen species, SARS-CoV=severe acute respiratory syndrome-corona virus, siRNA=small interfering RNA, SS=sodium salicylate, TRIF=Toll/IL-1R domain-containing adaptor-inducing IFN-β, Vpr-viral protein R, WB=Western blot

The online version of this paper, found at www.jleukbio.org, includes supplemental information.

1. Correspondence: Research Institute, International Medical Center of Japan, 1-21-1 Toyama, Shinjuku-ku, Tokyo 162-8655, Japan. E-mail: zakay@ri.imcj.go.jp

[14]. Exogenous Vpr induces apoptosis in T cells and neurons as a result of its toxic effects on mitochondria [15, 16], and we found recently that even small amounts of Vpr attenuated neurite outgrowth by inducing mitochondrial dysfunction [17]. It is well accepted that HIV-1-positive patients suffer from functional defects of the CNS [18]. Additionally, Deshmane et al. [19] demonstrated recently that HIF-1, a biomarker of oxidative stress, was expressed in the brain tissue of patients with HIV-1-associated dementia. Additional experiments involving the expression of Vpr in human microglial cells revealed that Vpr generated ROS with concomitant HIF-1 expression. These observations suggest that mitochondrial dysfunction as well as oxidative stress as a result of Vpr comprise the molecular basis for AIDS-associated clinical symptoms [20, 21].

TLRs, which are involved in the first line of defense against pathogens and microorganisms in macrophages and dendritic cells [22, 23], function as pattern-recognition receptors and recognize pathogen-associated molecules. To date, 13 TLR family members have been identified, and their modulation induces the production of various inflammatory cytokines, chemokines, and IFNs [22, 23]. Of these, TLR2 and TLR4 recognize proteins derived from microorganisms; TLR2 recognizes the hemagglutinin protein of the measles virus, and TLR4 recognizes the envelope proteins of respiratory syncytial virus and mouse mammary tumor virus [22, 23]. TLR4 uses four adaptor proteins for intracellular signaling (TRIF-related adaptor molecule, TRIF, Mal, and MyD88), which activate MyD88-dependent and -independent pathways differentially in response to various pathogens [22, 23]. Cytokine production, reflecting the activation of effector molecules involved in innate immunity, is stimulated by the NF-κB and MAPK signaling pathways [24], which activate downstream transcription factors such as NF-κB, c-Jun, C/EBP-β, and CREB [24–26].

Recently, oxidative stress was shown to be linked to innate immunity [27]. OxPC, formed from phospholipids in response to oxidative stress, were identified originally in atherosclerotic lesions. Imai et al. [27] showed recently that OxPC was formed during infection with SARS-CoV or H5N1 and that it induced TLR4-mediated IL-6 production. Furthermore, E06, a mAb against OxPC, ameliorated pathological changes in lung tissue, implying that OxPC formation is a critical factor responsible for the severe clinical course caused by these viruses [27]. Importantly, recent observations have suggested that oxidative stress is involved in a variety of pathological conditions, including diabetes mellitus [28] and neurodegenerative diseases such as Alzheimer's disease [29] and Parkinson's disease

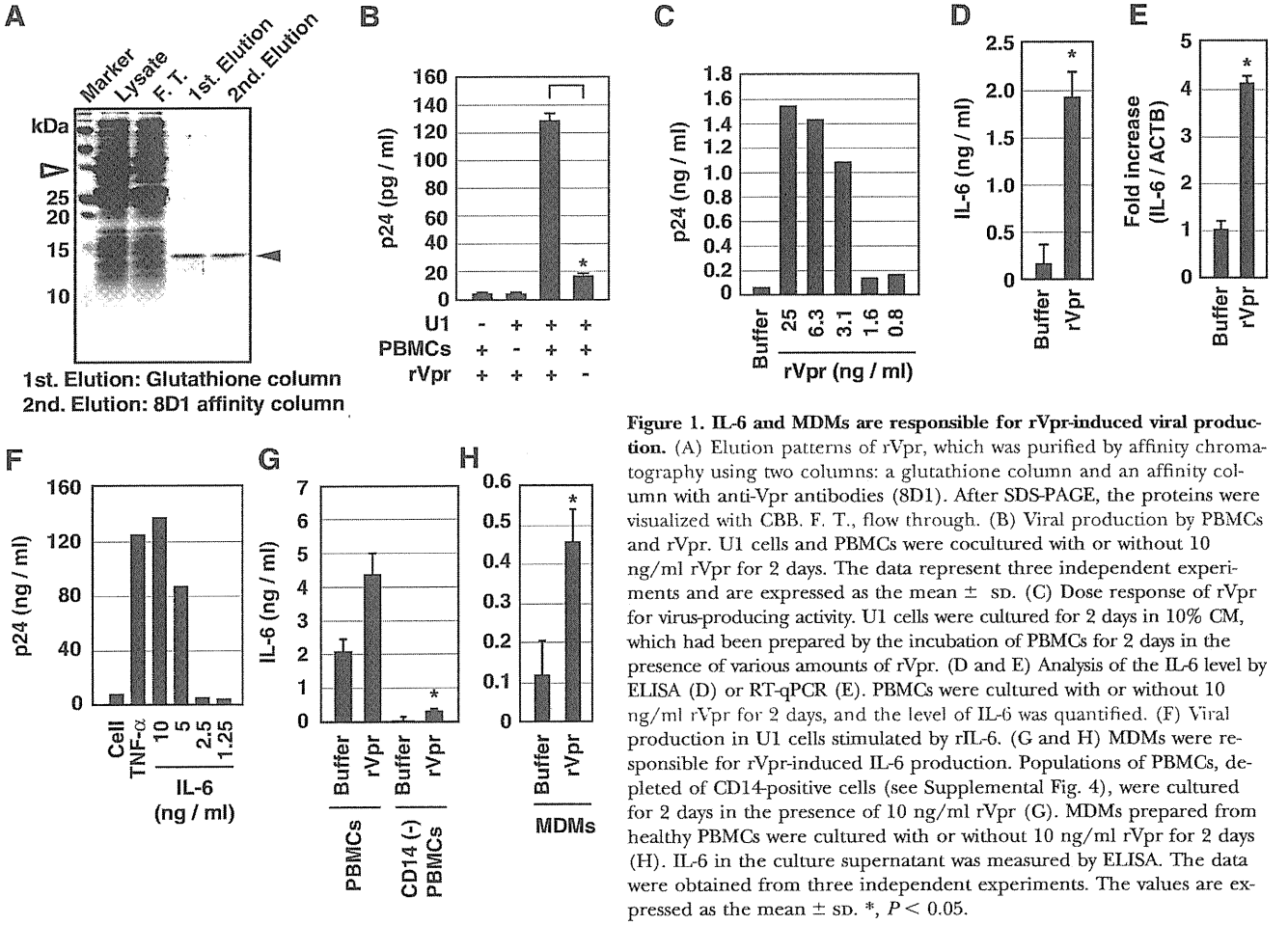

Figure 1. IL-6 and MDMs are responsible for rVpr-induced viral production. (A) Elution patterns of rVpr, which was purified by affinity chromatography using two columns: a glutathione column and an affinity column with anti-Vpr antibodies (8D1). After SDS-PAGE, the proteins were visualized with CBB. F. T., flow through. (B) Viral production by PBMCs and rVpr. U1 cells and PBMCs were cocultured with or without 10 ng/ml rVpr for 2 days. The data represent three independent experiments and are expressed as the mean ± SD. (C) Dose response of rVpr for virus-producing activity. U1 cells were cultured for 2 days in 10% CM, which had been prepared by the incubation of PBMCs for 2 days in the presence of various amounts of rVpr. (D and E) Analysis of the IL-6 level by ELISA (D) or RT-qPCR (E). PBMCs were cultured with or without 10 ng/ml rVpr for 2 days, and the level of IL-6 was quantified. (F) Viral production in U1 cells stimulated by rIL-6. (G and H) MDMs were responsible for rVpr-induced IL-6 production. Populations of PBMCs, depleted of CD14-positive cells (see Supplemental Fig. 4), were cultured for 2 days in the presence of 10 ng/ml rVpr (G). MDMs prepared from healthy PBMCs were cultured with or without 10 ng/ml rVpr for 2 days (H). IL-6 in the culture supernatant was measured by ELISA. The data were obtained from three independent experiments. The values are expressed as the mean ± SD. *, $P < 0.05$.

[30]. It is therefore important to clarify the possible link between the inappropriate activation of innate immune responses and the development of intractable human diseases.

Here, we show that rVpr induced the formation of OxPC in MDMs and that this induction was blocked by the addition of NAC, a scavenger of ROS. An analysis of signaling cascades revealed that rVpr activated the TLR4/MyD88 pathway and consequently modulated the NF-κB and MAPK pathways as a downstream effect. Interestingly, an antibody against OxPC (DLH3) attenuated rVpr-induced IL-6 production and the phosphorylation of C/EBP-β, suggesting that the formation of OxPC is involved as a pan upstream event in Vpr-induced IL-6 production. Along with evidence that rVpr, added exogenously at a concentration comparable with that observed in patient plasma, reactivated viral reproduction via IL-6 production, we propose that the monitoring of Vpr in the context of clinical outcome is important for understanding the mechanism of recurrent viral production in patients; moreover, our data provide the rationale for the development of novel anti-AIDS therapeutics targeting Vpr.

MATERIALS AND METHODS

Cells and chemicals

Peripheral blood was donated by healthy humans who worked within the institute and gave informed consent. The ethics committee of the institute approved the current project designed to clarify the role of Vpr in AIDS development. Mononuclear cells (PBMCs) were prepared from the peripheral blood by using Lymphoprep (Axis-Shield, Dundee Technology Park, Dundee, Scotland), and then monocytes were isolated from the PBMCs via CD14-negative selection using a magnetic cell sorting (MACS) system (Miltenyi Biotec, Bergisch Gladbach, Germany). For preparation of MDMs, recovered monocytes were cultured for 4 days with M-CSF (50 ng/ml; R&D Systems, Minneapolis, MN, USA). In the CD14-depletion experiment, PBMCs were treated with magnetic beads conjugated with anti-CD14 antibody (Miltenyi Biotec). Human U1 cells [4], a monocytic cell line of HIV-1 latently infected cells, were provided by National Institutes of Health AIDS (Germantown, MD, USA). The PBMCs, MDMs, and U1 cells were cultured in RPMI 1640 containing 10% FCS at 37°C and 5% CO_2. In the complementation experiment of C/EBP-β, THP-1 was cultured in IMDM with 10% FCS at 37°C and 5% CO_2. To investigate any indirect effects of Vpr against latently infected cells, we performed coculture experiments. For these, the U1 cells and PBMCs were cultured using a noncontact cell coculture insert system (BD Falcon, Franklin Lakes, NJ, USA) in RPMI 1640 with 10% FCS at 37°C and 5% CO_2. The calpain I inhibitor ALLN, the p38 MAPK inhibitor 4-(4-fluorophenyl)-2-(4-hydroxyphenyl)-5-(4-pyridyl)-1H-imidazole (SB202190), and the IKK inhibitor SS were purchased from Sigma Chemical Co. (St. Louis, MO, USA).

Purification of rVpr

rVpr and ΔC12, a deletion mutant of the C-terminal 12 aa of rVpr, were expressed as a GST fusion protein in BL21-CodonPlus (DE3; Stratagene, La Jolla, CA, USA) and purified using a two-step affinity column chromatography method with glutathione and anti-Vpr antibody beads, as described previously [13]. Briefly, GST-Vpr was first bound to a glutathione column,

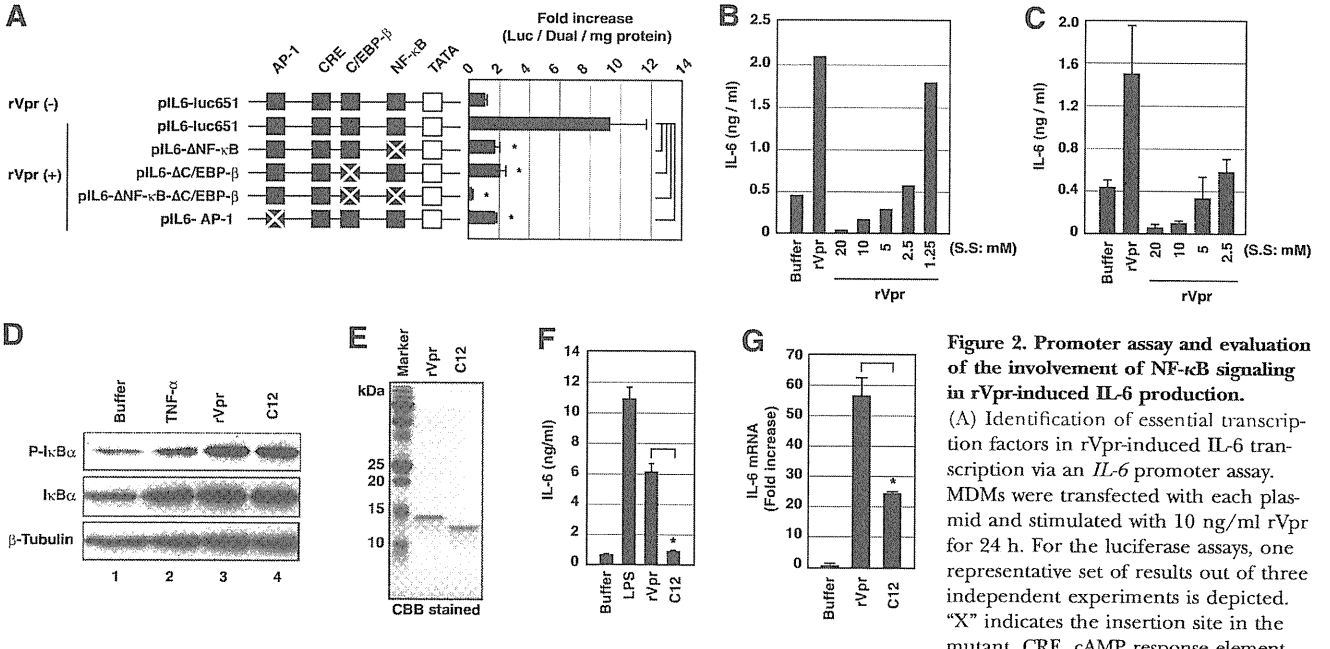

Figure 2. Promoter assay and evaluation of the involvement of NF-κB signaling in rVpr-induced IL-6 production. (A) Identification of essential transcription factors in rVpr-induced IL-6 transcription via an *IL-6* promoter assay. MDMs were transfected with each plasmid and stimulated with 10 ng/ml rVpr for 24 h. For the luciferase assays, one representative set of results out of three independent experiments is depicted. "X" indicates the insertion site in the mutant. CRE, cAMP response element. (B and C) Evaluation of the role of NF-κB in rVpr-induced IL-6 production. PBMCs (B) and MDMs (C) were pretreated with SS (1.25–20 mM) for 30 min and then cultured with or without 10 ng/ml rVpr for 2 days. PBMCs and MDMs were treated for 2 days before analysis by ELISA. The data shown in B were obtained from a single sample, whereas those shown in C were obtained from triplicate experiments for each sample. (D) ΔC12-induced IκB-α phosphorylation. MDMs were treated with or without stimulators (10 ng/ml TNF-α, rVpr, or ΔC12) for 40 min. Phosphorylated IκB-α (P-IκB-α) and total IκB-α were analyzed by WB. β-Tubulin was used as a loading control. (E) Purity of rVpr and ΔC12. The electrophoretic patterns of the purified proteins were visualized by CBB staining. (F and G) IL-6 was assayed after the treatment of cells with rVpr and ΔC12 at 10 ng/ml for 2 days prior to ELISA (F) and for 3 h prior to RT-qPCR (G). IL-6 production was tested in MDMs. The data were obtained from three independent experiments. The values are expressed as the mean ± SD. *, $P < 0.05$.

and Vpr proteins were cleaved from GST using PreScission (GE Healthcare, Milwaukee, WI, USA) and eluted with buffer [20 mM phosphate buffer (pH 7.6), 150 mM NaCl, 10% glycerol, 1 mM PMSF, 0.1% Triton X-100]. The eluted rVpr was then applied to an affinity column containing two kinds of mAb against rVpr (8D1 and C217). After washing the column thoroughly using buffer prepared with pyrogen-free distilled water, the rVpr proteins were eluted with 100 mM HEPES (pH 2.5). The eluate containing rVpr or ΔC12 (see Fig. 2E) was neutralized immediately by 1 M HEPES (pH 7.6). As LPS could have contaminated the purified rVpr solution, we tested for the presence of LPS using a highly sensitive LPS assay with LAL, the detection limit of which was 0.001 EU/ml (Endospecy kit and Toxicolor DIA kit, Seikagaku Corp., Tokyo, Japan; Supplemental Fig. 1A). rVpr, purified by an affinity column chromatography with 8D1, contained no detectable LPS (Supplemental Fig. 1A). We also confirmed that the purified rVpr solution did not inhibit the detection of LPS (data not shown). The activity of rVpr was abolished completely with heat for 5 min (boiling at 100°C). In contrast, the activity of LPS was partially restored (Supplemental Fig. 1B).

Detection of IL-6 and p24

Cells were cultured for 2 days with rVpr (10 ng/ml) or LPS (10 pg/ml; Sigma Chemical Co.). We analyzed IL-6 and p24, a HIV-1 capsid protein, in the culture supernatants using IL-6 (Endogen, Pierce, Rockford, IL, USA) and p24 (ZeptoMetrix, Buffalo, NY, USA) ELISA kits, respectively. The cells were cultured with stimuli for 3 h, and then, the mRNA for RT-qPCR was prepared using an RNeasy Mini kit (Qiagen, Valencia, CA, USA). The RT reaction was performed using a ReverTra Ace qPCR RT kit (Toyobo, Osaka, Japan) following the manufacturer's instructions. The qPCR was performed using ABI prism 7000 (Applied Biosystems, Foster City, CA, USA) and TaqMan Gene Expression Assays (Applied Biosystems).

Protein array and WB analyses

The PBMCs were cultured with or without rVpr for 2 days, and the culture supernatants were analyzed using a protein array system (TranSignal Human Cytokine Antibody Array 1.0, Panomics, Redwood City, CA, USA). Various cytokines and chemokines were identified using specific antibodies plotted on membranes. To detect the phosphorylation of IκB-α, the MDMs were pretreated with ALLN (150 μM; Sigma Chemical Co.) for 2 h and then treated with rVpr for 40 min. To analyze the phosphorylation of C/EBP-β and c-jun, the MDMs were exposed to rVpr for 40 min. The MDMs were then lysed with RIPA buffer [50 mM Tris–HCl (pH 8.0), 150 mM NaCl, 0.1% SDS, 0.5% sodium deoxycholate, 1% Nonidet P-40, protease inhibitor cocktail (Roche Diagnostics, Basel, Switzerland), 10 mM β-glycerophosphate, 1 mM Na_3VO_4, 5 mM pixels per inch, and 50 mM NaF], and the cell lysates were subjected to SDS-PAGE. For these experiments, we used antibodies against phosphorylated IκB-α, C/EBP-β, and c-jun, their regular forms (Cell Signaling Technology, Danvers, MA, USA), and β-tubulin (NeoMarkers, Lab Vision, Fremont, CA, USA).

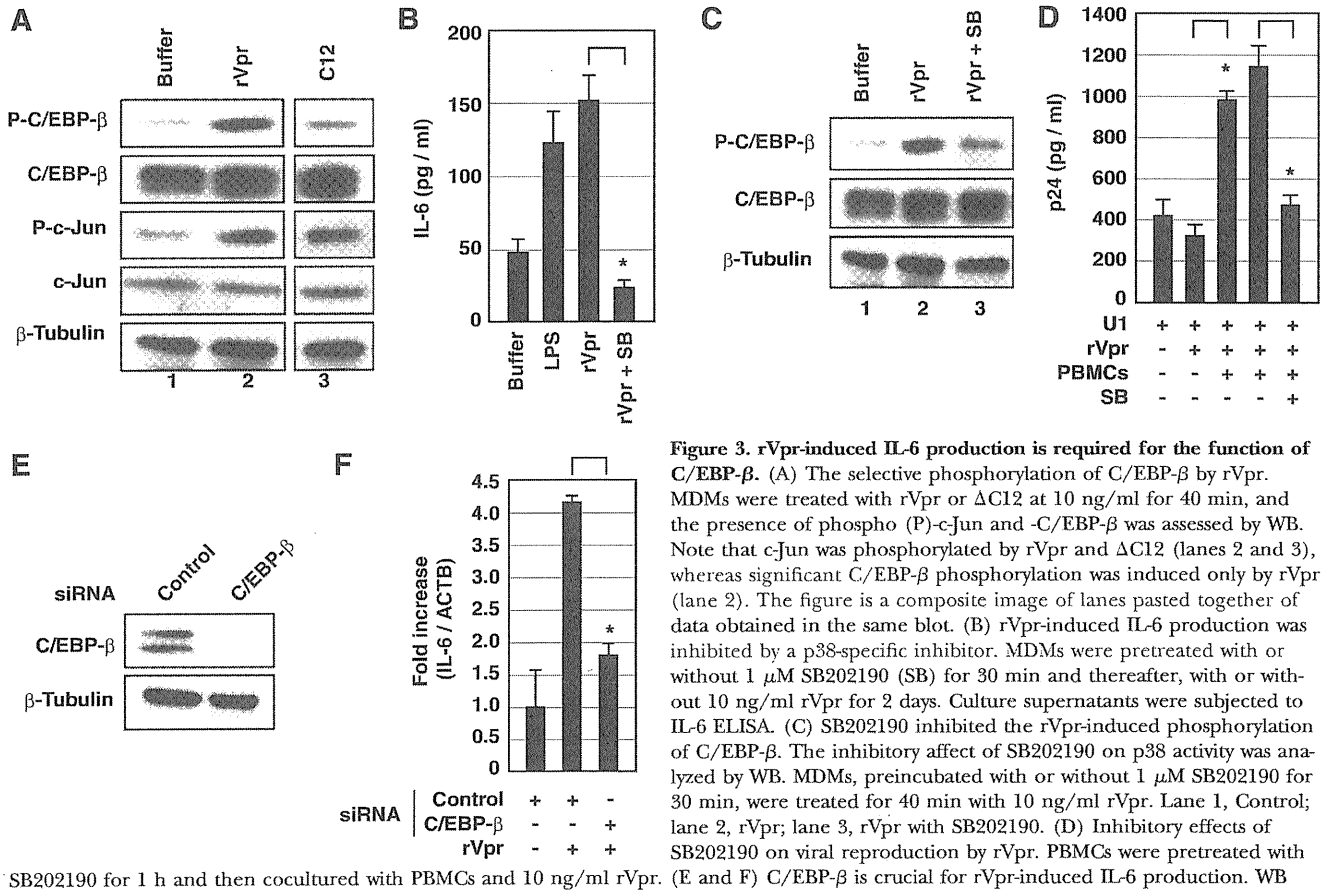

Figure 3. rVpr-induced IL-6 production is required for the function of C/EBP-β. (A) The selective phosphorylation of C/EBP-β by rVpr. MDMs were treated with rVpr or ΔC12 at 10 ng/ml for 40 min, and the presence of phospho (P)-c-Jun and -C/EBP-β was assessed by WB. Note that c-Jun was phosphorylated by rVpr and ΔC12 (lanes 2 and 3), whereas significant C/EBP-β phosphorylation was induced only by rVpr (lane 2). The figure is a composite image of lanes pasted together of data obtained in the same blot. (B) rVpr-induced IL-6 production was inhibited by a p38-specific inhibitor. MDMs were pretreated with or without 1 μM SB202190 (SB) for 30 min and thereafter, with or without 10 ng/ml rVpr for 2 days. Culture supernatants were subjected to IL-6 ELISA. (C) SB202190 inhibited the rVpr-induced phosphorylation of C/EBP-β. The inhibitory affect of SB202190 on p38 activity was analyzed by WB. MDMs, preincubated with or without 1 μM SB202190 for 30 min, were treated for 40 min with 10 ng/ml rVpr. Lane 1, Control; lane 2, rVpr; lane 3, rVpr with SB202190. (D) Inhibitory effects of SB202190 on viral reproduction by rVpr. PBMCs were pretreated with SB202190 for 1 h and then cocultured with PBMCs and 10 ng/ml rVpr. (E and F) C/EBP-β is crucial for rVpr-induced IL-6 production. WB was performed on MDMs that had been transfected with C/EBP-β siRNA. Endogenous C/EBP-β expression was down-regulated efficiently (lane 2; E). β-Tubulin was included as a loading control. The activity of rVpr (10 ng/ml for 40 min) was examined in these cells by RT-qPCR (F). The level of *IL-6* mRNA was normalized to ACTB. The data were obtained from three independent experiments. The values are expressed as the mean ± SD. *, $P < 0.05$.

Blocking experiments

The PBMCs were treated with rVpr for 2 days, and the collected culture supernatants were treated with anti-IL-6 antibody (R&D Systems) or control mouse IgG (Sigma Chemical Co.). The U1 cells were cultured in RPMI 1640 containing 10% antibody-treated culture supernatant of PBMCs, which were treated with rVpr for an additional 2 days, and the culture supernatants were analyzed for virus production using p24 ELISA. For blocking experiments, PBMCs were pretreated with 8D1 or control IgG for 30 min and then cultured for 2 days in the absence or presence of rVpr (10 ng/ml). Thereafter, culture supernatants were harvested, and IL-6 concentration was analyzed by ELISA. To determine the involvement of TLRs with rVpr-induced IL-6 production, we pretreated the MDMs with anti-TLR2 (Abcam, Cambridge, MA, USA) and anti-TLR4 (Abcam) antibodies for 20 min and then treated the MDMs with rVpr for 3 h. Subsequently, we measured the level of IL-6 mRNA expression using RT-qPCR.

Inhibitor experiments

The PBMCs and MDMs were pretreated with SS (1.25–20 mM) or SB202190 (1 μM) for 30 min before the addition of rVpr. After 2 days, the cultured supernatants were collected and analyzed for IL-6 concentration using an IL-6 ELISA. To test the effects on rVpr-induced virus reproduction, the PBMCs were pretreated with SB202190 (1 μM) for 1 h and then exposed to rVpr overnight. Subsequently, the U1 cells were cocultured with SB202190 and treated with rVpr PBMCs for 2 additional days. The virus concentrations were analyzed in the culture supernatants using the p24 ELISA. NAC (20 mM; Sigma Chemical Co.) [31], a scavenger of ROS, was added to MDMs for 30 min; then, rVpr was treated for 2 days (ELISA) or for 40 min (WB) with NAC. The culture media or the cell lysates were subjected to analysis of IL-6 by ELISA or phosphorylation of IκB-α, c-jun, and C/EBP-β by WB.

Promoter assay

We measured the transcriptional activity of the IL-6 promoter using the following reporter plasmids: pIL6-luc651, pIL6-ΔNF-κB, pIL6-ΔC/EBP-β, pIL6-ΔNF-κB-ΔC/EBP-β, and pIL6-ΔAP-1 [32]. Each reporter construct had been mutated to exclude one or two transcription factor-binding sites and to encode firefly luciferase as the reporter gene. Dr. Oliver Eickelberg (University of Giessen, Germany) kindly provided these reporter plasmids. The MDMs (5×10^5 cells) were cotransfected with 2 μg each pIL6-luc651 and their mutant plasmid DNA, with 0.5 μg *Renilla reniformis* luciferase expression plasmid DNA as an internal control (pGL4.73; Promega, Madison, WI, USA). Lipofectamine 2000 (Invitrogen, Carlsbad, CA, USA) was used for transfecting the plasmids into the MDMs. The following day, the MDMs were treated with rVpr for 24 h, and luciferase activity was measured using PicaGene (Toyo Ink, Tokyo, Japan). The luciferase activities in the cell lysates were normalized using the protein concentration measured with a bicinchoninic acid protein assay kit (Thermo Scientific, Fremont, CA, USA).

RNA interference and complementation experiments

siRNAs were used to block C/EBP-β, MyD88, and TLR4 expression (C/EBP-β; Ambion, Foster City, CA, USA; MyD88 and TLR4, Dharmacon, Fremont, CA, USA). Sequences of each siRNA were C/EBP-β: 5′-CCCACGUGUAACUGUCAGCtt-3′, 5′-CCAACCGCACAUGCAGAUGtt-3′, and 5′-GCCCGUCGGUAAUUUUAAUtt-3′; MyD88: 5′-CGACUGAAGUUGUGUGUGU-3′, 5′-GCUAGUGAGCUCAUCGAAA-3′, 5′-GCAUAUGCCUGAGCGUUUC-3′, and 5′-GCACCUGUGUCUGGUCUAU-3′; and TLR4: 5′-UGGUGGAAGUUGAACGAAU-3′, 5′-GUUUAGAAGUCCAUCGUUU-3′, 5′-CAUUGAAGAAUUCCGAUUA-3′, and 5′-GGAAAAUGGUGUAGCCGUU-3′. As control, a mixture of three irrelevant siRNAs with nontargeting sequences was used [*Silencer* Negative Control Nos. 1–3 siRNA (Catalog No. 1: AM4611, No. 2: AM4613, No. 3: AM4615); Ambion]. Each control sequence was a nondisclosure by the manufacturer's policy.

The MDMs were transfected with 100 pmoles siRNA molecules using Lipofectamine 2000 and were cultured for 2 days before the cell lysates were prepared using RIPA buffer. To confirm the effects of the siRNAs, the protein expression levels of endogenous C/EBP-β and MyD88 were examined using antibodies specific for α-C/EBP-β and α-MyD88 (Cell Signaling Technology). The repression of TLR4 was confirmed by determining the mRNA expression level and immunostaining. The primer sequences used for RT-PCR detection of TLR4 were 5′-CGGATGGCAACATTTAGAATTAGT-3′ (forward) and 5′-TGATTGAGACTGTA-ATCAAGAACC-3′ (reverse). To confirm the knockdown of endogenous TLR4, immunostaining was performed using an antibody against TLR4 (HTA125; Abcam). The MDMs transfected with TLR4 siRNA were washed once with cold PBS and incubated with PBS containing 10% FCS, 0.5% NaN_3, and 1 mM PMSF for 10 min at 4°C. Subsequently, the MDMs were washed with cold PBS and treated for 1 h at 4°C using 1 μg α-TLR4 antibody (Abcam) diluted with PBS containing 0.2% NaN_3 and 3% BSA. After 1 h, the MDMs were washed three times with cold PBS and fixed with 0.5% PFA for 15 min. Subsequently, TLR4 was detected using α-mouse IgG-Alexa-546 (Invitrogen) as the secondary antibody.

In the C/EBP-β complementation experiment, the C/EBP-β cDNA was cloned using macrophages obtained from healthy volunteers and then inserted into an expression plasmid. The THP-1 cells were transfected with 2.5 μg C/EBP-β expression plasmid using 2 μl Lipofectamine 2000 in 500 μl Opti-MEM. After 2 days, the cells were collected and lysed with RIPA buffer. The lysate was analyzed to determine the expression level of exogenous C/EBP-β by WB analysis. The transfectant was stimulated with rVpr or LPS for 3 h. We then prepared RT-qPCR samples using a RNA extraction kit (Qiagen). The IL-6 expression level was analyzed using a RT-qPCR system.

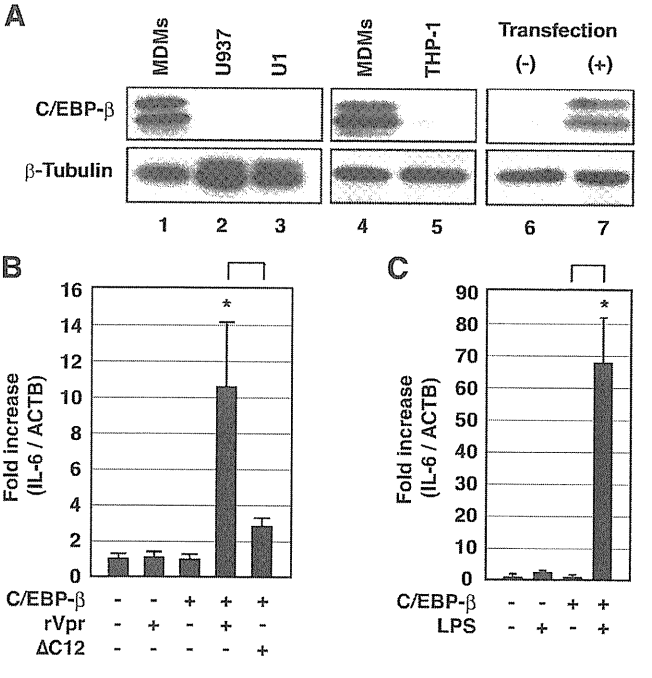

Figure 4. C/EBP-β is essential for rVpr-induced IL-6 production. (A) Weak expression of endogenous C/EBP-β in leukemic cells. WB was performed using MDMs and U1, U937, or THP-1 cells (lanes 1–5) and THP-1 cells transfected with exogenous *C/EBP-β* cDNA (lanes 6 and 7). β-Tubulin was included as a loading control. (B) The response to rVpr was restored by C/EBP-β. After transfection with *C/EBP-β* cDNA, THP-1 cells were cultured with rVpr or ΔC12 at 10 ng/ml, and *IL-6* mRNA expression was analyzed. (C) LPS activated THP-1 cells dramatically after the introduction of *C/EBP-β* cDNA. LPS was added for 3 h at 10 ng/ml, and *IL-6* mRNA expression was analyzed by RT-qPCR. The data were obtained from three independent experiments. The values are expressed as the mean ± SD. *, $P < 0.05$.

JLB

Detection of MMP and oxidized phospholipids

The MDMs were first treated for 15 min with rVpr and then with 5 μg/ml Rhodamine 123 (Sigma Chemical Co.) for another 15 min. Then, cells were washed with cold PBS and subjected to analysis of MMP by a LSC system (Olympus, Tokyo, Japan). For immunostaining of OxPC, the cells were washed with cold PBS and fixed using 4% PFA. After fixation, the cells were blocked with 3% BSA containing PBS. Thereafter, the OxPC-specific mAb DLH3 [33, 34] was treated. As a control, a mAb of isotyped IgM (Rockland Immunochemicals, Philadelphia, PA, USA) was used. Then, an Alexa-555-labeled anti-mouse IgM (Invitrogen) as a secondary antibody was treated for 1 h at room temperature. Nuclear DNA was stained with Hoechst 33342 (Invitrogen).

For the blocking experiments, we cultured the MDMs with control IgM or DLH3 (5 nM) for 20 min and then added rVpr and the primary antibodies (20 nM) and cultured these for 30 min. We then collected IL-6 mRNA and analyzed these molecules using qPCR. For the immunostaining experiments, we fixed the cells with cold methanol and blocked them with 5% BSA containing PBS. Thereafter, the anti-C/EBP-β antibody (Cell Signaling Technology) was used as a primary antibody, and Alexa-546-labeled anti-rabbit IgG (Invitrogen) was used as a secondary antibody. Nuclear DNA was stained with Hoechst 33342 (Invitrogen).

Biacore system

The possible interaction of rVpr and a rTLR4 protein was examined by using the Biacore J system (GE Healthcare). rVpr were coupled with sensor chip CM5 (GE Healthcare; BR-1005-30) by the amine coupling kit (GE Healthcare; BR-1000-10), and soluble TLR4, which was expressed by the baculovirus system and purified as described [35], was used as an analyte. Binding analysis of binding was done, following the manufacturer's instructions.

Statistical analysis

Data were generated from at least three replicate experiments. The statistical analysis was conducted by the Mann-Whitney U test. A P value of <0.05 was considered to be statistically significant.

RESULTS

IL-6 production from MDMs is stimulated by rVpr

We reported previously that the maximum concentration of Vpr present in patient plasma was ~5 ng/ml (0.3 nM) [13]. Thus, we thought it reasonable to investigate the biological activity of exogenous rVpr added at the ng/ml level. We first examined the activity of highly purified rVpr, which was prepared by affinity column chromatography using a mAb against rVpr (8D1; **Fig. 1A**). Following the addition of purified rVpr (Supplemental Fig. 1, A and B) to latently infected U1 cells [4], remarkable viral reproduction was observed when the cells were cocultured with PBMCs ($P<0.05$; Fig. 1B). In contrast, rVpr alone induced no reproductive activity in U1 cells (Fig. 1B, second column from the left, and Supplemental Fig. 2). CM prepared from PBMCs cultured with rVpr for 2 days also showed viral reproductive activity (Fig. 1C), suggesting that rVpr stimulates PBMCs to generate a humoral factor(s) that induces viral reproduction in U1 cells. Note that even 3 or 6 ng/ml rVpr, which is comparable with the concentration present in the plasma of HIV-1-positive patients, induced viral reproduction (Fig. 1C). To characterize the factors responsible for viral production, CM was prepared from the PBMCs of three healthy volunteers and subjected to protein array analysis (Supplemental Fig. 3). Among the factors tested, IL-6 was selected as a candidate, as its production was reproducibly correlated with the level of rVpr-induced viral production. Consistent with this, anti-IL-6 antibodies blocked the viral induction activity of the CM (Supplemental Table 1), suggesting that the factor responsible for the rVpr-induced reactivation of viral production was IL-6.

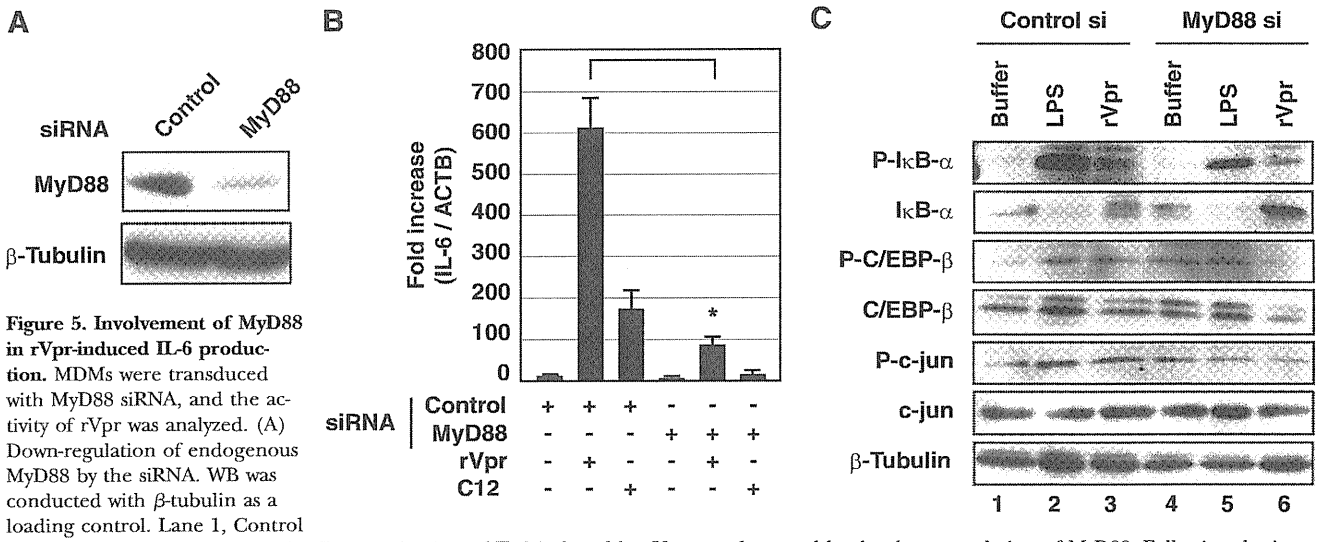

Figure 5. Involvement of MyD88 in rVpr-induced IL-6 production. MDMs were transduced with MyD88 siRNA, and the activity of rVpr was analyzed. (A) Down-regulation of endogenous MyD88 by the siRNA. WB was conducted with β-tubulin as a loading control. Lane 1, Control siRNA; lane 2, MyD88 siRNA. (B) The production of IL-6 induced by rVpr was abrogated by the down-regulation of MyD88. Following the introduction of MyD88 siRNA, MDMs were treated with rVpr or ΔC12 at 10 ng/ml. IL-6 production was then measured by RT-qPCR. *, $P < 0.05$. (C) Involvement of the MyD88-independent pathway in rVpr-induced IL-6 production. After the introduction of MyD88 siRNA (si), MDMs were treated for 40 min with 10 ng/ml rVpr or 10 pg/ml LPS, and the phosphorylation of each transcription factor was analyzed by WB. Lanes 1–3 represent control siRNA-treated cells, and lanes 4–6 represent cells treated with MyD88 siRNA. Lanes 1 and 4, Buffer control; lanes 2 and 5, LPS; lanes 3 and 6, rVpr. β-Tubulin was included as a loading control. MyD88 siRNA inhibited LPS-induced IL-6 production. LPS was added at 10 pg/ml for 3 h, and the expression of IL-6 in MDMs was analyzed by RT-qPCR. The data were obtained from three independent experiments. The values are expressed as the mean ± SD.

TABLE 1. Effects of Anti-TLR4 on Vpr-Induced IL-6 Production

Stimulators	W/o IgG	IgG		
		Control	α-TLR2	α-TLR4
None	1.0 ± 0.83	2.3 ± 1.38	2.2 ± 0.34	0.5 ± 0.32
rVpr	40.5 ± 10.8	37.0 ± 6.75[a]	40.1 ± 18.4	19.9 ± 9.78[a]

(Fold increase). [a]$P < 0.05$. Each antibody was added to MDMs cultured in the presence of rVpr, and then, IL-6 in the supernatant was measured by IL-6 ELISA. Of note, α-TLR4 inhibited IL-6 production from MDMs stimulated by LPS. W/o, Without.

To confirm that IL-6 was induced by rVpr, we measured IL-6 directly. Analysis by ELISA and RT-qPCR revealed that the addition of rVpr to MDMs induced the production of IL-6 significantly ($P<0.05$; Fig. 1, D and E). Additionally, we found that a comparable amount of rIL-6 induced viral reproduction in a dose-dependent manner (Fig. 1F). Next, to identify the cells responsible for rVpr-induced IL-6 production, we performed fractionation experiments using an antibody against CD14, a monocyte marker. We first removed all CD14-positive cells from the PBMCs. The recovered cells (Supplemental Fig. 4) were then cultured in the presence of rVpr. As shown in Figure 1G, no IL-6 production was observed following the addition of rVpr to the CD14-negative cell fraction ($P<0.05$; Fig. 1G). In contrast, the CD14-positive cells recovered from the MDMs showed vigorous IL-6 production in response to rVpr ($P<0.05$; Fig. 1H). These data indicate that rVpr-induced IL-6 production is dependent on monocytes/MDMs and that IL-6 is a mediator of rVpr-induced viral reproduction.

As our findings for rVpr were similar to those obtained with LPS, we performed additional experiments. First, we detected no LPS using the LAL test, a highly sensitive method with a detection limit of 0.001 EU/ml LPS (Supplemental Fig. 1A). Second, the activity of rVpr was abolished completely by boiling for 5 min, whereas that of LPS was reduced only partially following the same procedure (Supplemental Fig. 1B). Additionally, Vpr-induced IL-6 production was eliminated by pretreatment with a mAb against Vpr but not by control IgG (Supplemental Fig. 5). These results support the idea that the activation of MDMs by IL-6 represents authentic Vpr activity. We therefore sought to further characterize the signaling cascades induced by rVpr.

NF-κB activation is required for rVpr-induced IL-6 production

The *IL-6* promoter contains binding sites for four transcription factors: NF-κB, C/EBP-β, CREB, and AP-1. To identify the transcription factor(s) essential for rVpr-induced *IL-6* mRNA production, we performed a promoter assay using firefly *luciferase* as a reporter gene and observed that rVpr increased the activity of the *IL-6* promoter (**Fig. 2A**). In contrast, mutations in each IL-6 transcription factor-binding site markedly diminished *IL-6* promoter activity ($P<0.05$; Fig. 2A), suggesting that all of the transcription factors examined are required for rVpr-induced IL-6 production.

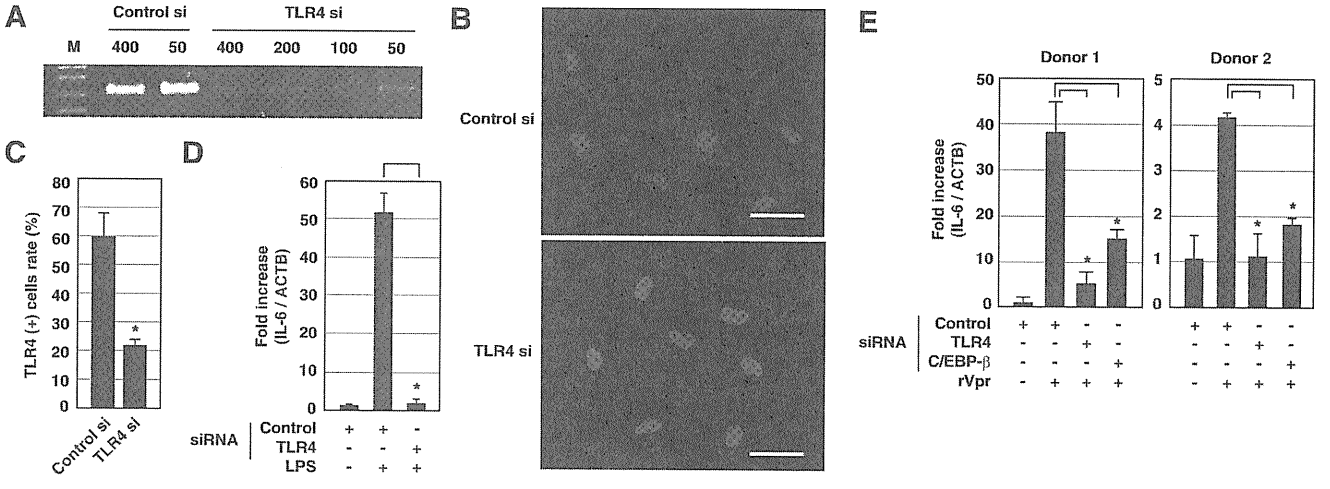

Figure 6. Involvement of TLR4 in rVpr-induced IL-6 production. MDMs were transfected with TLR4 siRNA, and their reactivity to rVpr was analyzed. The knockdown of endogenous TLR4 was confirmed by RT-PCR (A) and immunofluorescent staining (B; red, TLR4; blue, nucleus; original scale bars, 10 μm). M, marker. (C) TLR4 siRNA decreased the number of TLR4-positive cells, and the positive cells in the samples with the control and TLR4 siRNAs were counted. (D and E) The response to LPS or rVpr by cells with down-regulated TLR4. MDMs induced with TLR4 siRNA were treated with 10 pg/ml LPS (D) or 10 ng/ml rVpr (E) for 3 h. Following siRNA treatment, *IL-6* mRNA expression was analyzed by RT-qPCR. Responsiveness to rVpr was examined in two healthy donors (Donors 1 and 2). The data were obtained from three independent experiments. The values are expressed as the mean ± SD. *, $P < 0.05$.

JLB

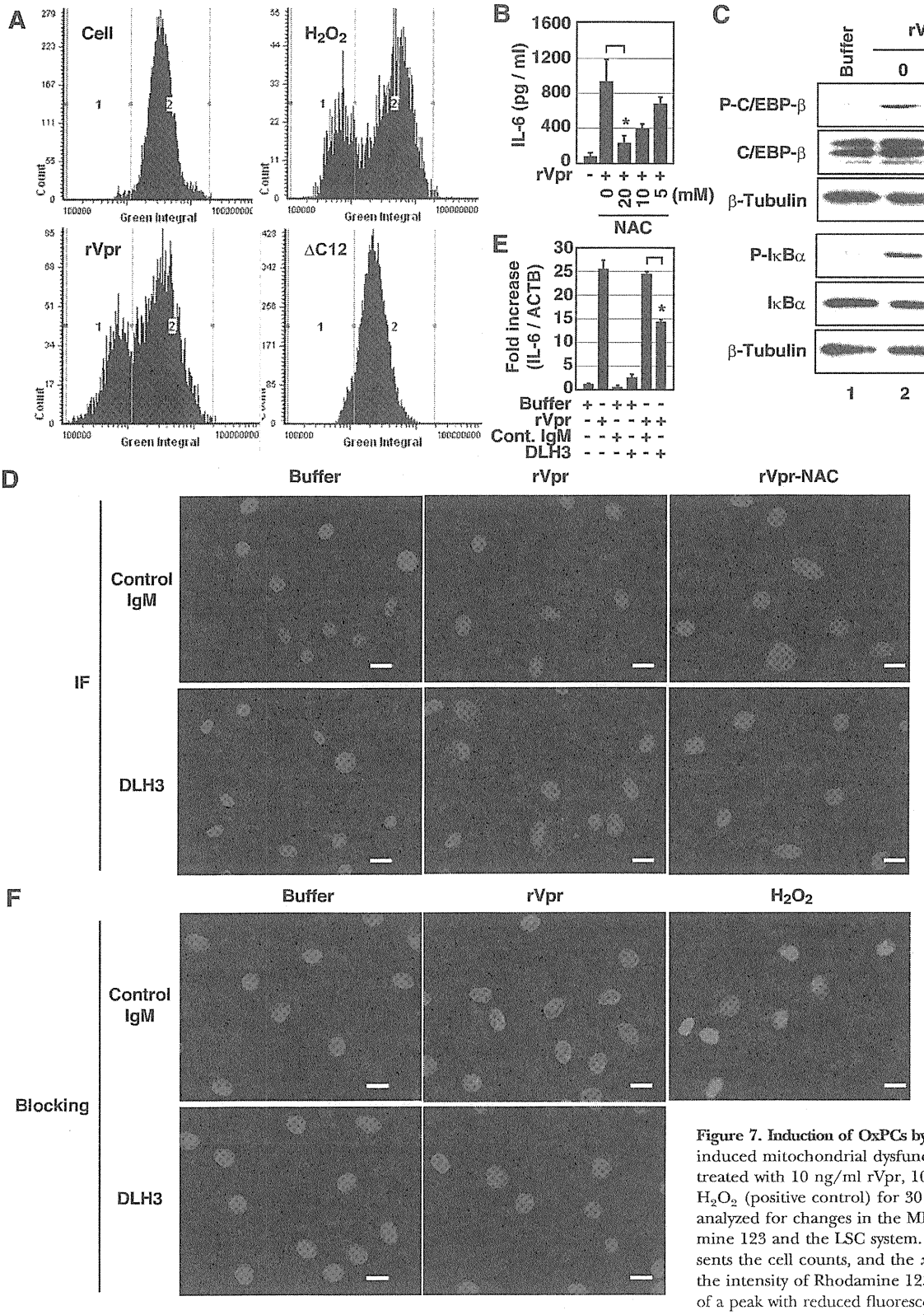

Figure 7. Induction of OxPCs by rVpr. (A) rVpr-induced mitochondrial dysfunction. MDMs were treated with 10 ng/ml rVpr, 10 ng/ml ΔC12, or H_2O_2 (positive control) for 30 min and then analyzed for changes in the MMP using Rhodamine 123 and the LSC system. The *y*-axis represents the cell counts, and the *x*-axis represents the intensity of Rhodamine 123. The presence of a peak with reduced fluorescence intensity indicates a decrease in the MMP [17]. (B) NAC inhibited rVpr-induced IL-6 production. MDMs were treated with NAC at 5, 10, or 20 mM in the presence of 10 ng/ml rVpr for 2 days. (C) The rVpr-induced phosphorylation of C/EBP-β and IκB-α was inhibited by NAC. MDMs were treated with 10 ng/ml rVpr in the presence (lane 3) or

(*continued on next page*)

As Vpr was reported to activate the NF-κB and MAPK pathways [36], we next examined the functional linkage of IκB-α phosphorylation with rVpr-induced IL-6 production. First, we observed that SS, a known inhibitor of IKK [37], blocked rVpr-induced IL-6 production from PBMCs (Fig. 2B) and MDMs (Fig. 2C). Consistent with this, we found that IκB-α was phosphorylated by rVpr (Fig. 2D, lane 3). To examine further the importance of IκB-α phosphorylation in *IL-6* transcription, we prepared a Vpr mutant lacking the ΔC12 (Fig. 2E). Previously, we found that the C-terminal region of Vpr was important for its function, and among several mutants lacking various lengths of the C-terminal region, ΔC12 was almost totally defective in terms of its biological activity compared with wild-type Vpr [38]. Compared with rVpr, ΔC12 showed significantly less ability to induce IL-6 production ($P<0.05$: Fig. 2, F and G). This mutant, however, induced the phosphorylation of IκB-α to a level comparable with that of rVpr (Fig. 2D, lane 4). These data indicate that rVpr-induced IL-6 production depends on the NF-κB pathway but that additional cellular factors are also required.

C/EBP-β is a pivotal factor in rVpr-induced IL-6 production

We next studied the involvement of AP-1 and C/EBP-β in rVpr-induced IL-6 production. WB analysis revealed that AP-1 was activated by rVpr and ΔC12 (**Fig. 3A**, middle column, lane 3), whereas C/EBP-β was activated selectively by rVpr (Fig. 3A, top column, lane 2). Additionally, SB202190, a specific inhibitor of p38, attenuated rVpr-induced IL-6 production ($P<0.05$; Fig. 3B, indicated by *) with concomitant inhibition of rVpr-induced C/EBP-β phosphorylation (Fig. 3C, lane 3). Moreover, SB202190 blocked viral production in U1 cells cocultured with PBMCs and rVpr ($P<0.05$; Fig. 3D). These observations indicate that C/EBP-β is a pivotal factor in rVpr-induced IL-6 production and viral production. To demonstrate this, we tested the effects of C/EBP-β siRNA on rVpr activity. Consistent with the data obtained using SB202190 (Fig. 3B), the knockdown of endogenous C/EBP-β expression abrogated rVpr-induced IL-6 production ($P<0.05$; Fig. 3, E and F).

To highlight further the importance of C/EBP-β in rVpr-induced IL-6 production, we conducted complementation experiments. As shown in **Figure 4A**, U1 (lane 3), its parental cell line U937 (lane 2), and THP-1 (lane 5), another human monocytic leukemia cell line, expressed low levels of endogenous C/EBP-β compared with MDMs (lanes 1 and 4). These three cell lines did not respond to rVpr by producing IL-6 (data not shown); however, the forced expression of exogenous *C/EBP-β* cDNA in leukemic cells (Fig. 4A, lane 7) made the cells competent for rVpr ($P<0.05$; Fig. 4B)- and LPS-induced IL-6 production ($P<0.05$; Fig. 4C). These results indicate that C/EBP-β is a pivotal factor in rVpr activity. Intriguingly, ΔC12 induced less IL-6, even under these conditions ($P<0.05$; Fig. 4B).

rVpr-induced IL-6 production depends on MyD88 and TLR4

To explore the involvement of the TLR signaling cascade in the modulation of NF-κB and MAPK by rVpr, we first examined the effects of the down-regulation of endogenous MyD88 on IL-6 production. The introduction of MyD88 siRNA into MDMs efficiently repressed endogenous MyD88 expression and responsiveness to LPS (**Fig. 5A** and Supplemental Fig. 6). Next, we examined the responsiveness to rVpr and found that rVpr-induced IL-6 production was attenuated significantly by the siRNA ($P<0.05$; Fig. 5B). We further characterized the phosphorylation status of several cellular proteins after the down-regulation of endogenous MyD88. Introduction of the siRNA reduced the rVpr-induced phosphorylation of IκB-α, C/EBP-β, and c-Jun significantly (Fig. 5C, compare lanes 3 and 6). Interestingly, the total amount of IκB-α was increased by rVpr (Fig. 5C, second column from the top, lane 6) but not by LPS. We obtained the same results in three independent experiments, suggesting that Vpr affects the processing of IκB-α, as postulated by Ayyavoo et al. [15].

Next, we examined the involvement of TLR molecules in this process. Among the TLR members tested, TLR2 and TLR4 were of primary interest, as these molecules were reported to interact with viral proteins [22, 23]. As an initial trial, we tested the effects of neutralizing antibodies against TLR2 and TLR4 and found that an anti-TLR4 antibody attenuated IL-6 production by rVpr ($P<0.05$; **Table 1**). We next analyzed the effects of TLR4 siRNA on rVpr-induced IL-6 production. The down-regulation of endogenous TLR4 was confirmed by RT-PCR (**Fig. 6A**), immunohistochemical analysis ($P<0.05$; Fig. 6, B and C), and LPS responsiveness testing ($P<0.05$; Fig. 6D). Two independent experiments were done using MDMs prepared from different healthy donors; both trials revealed that TLR4 siRNA attenuated rVpr-induced IL-6 production significantly ($P<0.05$; Fig. 6E).

rVpr-induced OxPC formation stimulates IL-6 production

Based on our results showing that rVpr-induced IL-6 production depended on TLR4/MyD88, we expected that rVpr would bind TLR4 directly. To demonstrate this, we examined the molecular interaction between rTLR4 proteins and rVpr using the Biacore system but obtained no positive results (data not shown). As another possibility, we hypothesized that TLR4/

absence (lanes 1 and 2) of 20 mM NAC. For the analysis of IκB-α, cells were treated with 150 μM ALLN. (D) Induction of OxPCs by rVpr. MDMs were treated with 10 ng/ml rVpr in the presence or absence of 20 mM NAC. Thereafter, the cells were fixed and stained using DLH3. Red, OxPCs; blue, nucleus; original scale bars, 10 μm. IF, immunofluorescence. (E) rVpr-induced IL-6 production was blocked by inhibiting the induction of OxPCs. MDMs were treated with 10 ng/ml rVpr in the presence or absence of 20 nM DLH3. mRNA samples were then collected, and the level of IL-6 expression was analyzed by RT-qPCR. ACTB was included as a loading control. (F) The rVpr-induced phosphorylation of C/EBP-β was blocked by inhibiting the induction of OxPCs. MDMs were treated with rVpr in the presence or absence of 20 nM DLH3. Thereafter, the cells were fixed and stained using α-phosphorylated C/EBP-β. Red, phosphorylated C/EBP-β; blue, nuclear DNA; original scale bars, 10 μm. The data were obtained from three independent experiments. The values are expressed as the mean ± SD. *, $P < 0.05$.

MyD88-dependent pathways were modulated by rVpr-induced oxidative stress and OxPC.

To investigate the involvement of OxPC in triggering rVpr-induced cellular responses, we first sought to determine whether IL-6 production was coupled with rVpr-induced oxidative stress by testing for changes in the MMP, an indicator of oxidative stress [17]. As observed in MDMs treated with H_2O_2 as a positive control (**Fig. 7A**, upper right panel), we found that rVpr generated a peak that was shifted to the left on the x-axis, indicating a decrease in the MMP (Fig. 7A, lower left panel; peak 1). In contrast, ΔC12 did not induce a shift (Fig. 7A, lower right panel; only peak 2 is observed). To show the importance of ROS in rVpr-induced IL-6 production, we next examined the effects of NAC on rVpr-induced cellular responses (Fig. 7B). As shown in Figure 7C, NAC decreased the rVpr-induced phosphorylation of C/EBP-β and IκB-α (Fig. 7C, compare lanes 2 and 3). We then examined the formation of OxPC following the addition of rVpr to MDMs. Interestingly, the mAb DLH3 [33, 34] detected OxPC, formed after treatment of rVpr (Fig. 7D, lower middle panel). The rVpr-induced formation of OxPC was blocked by the addition of NAC (Fig. 7D, lower right panel). Moreover, pretreatment of the MDMs with DLH3 attenuated rVpr-induced IL-6 production ($P<0.05$; Fig. 7E) and the phosphorylation of C/EBP-β (Fig. 7F, compare the upper middle and lower middle panels). These data suggest that OxPC, generated by rVpr-induced oxidative stress, modulate TLR4/MyD88 signaling and induce IL-6 production via the phosphorylation of C/EBP-β.

DISCUSSION

In this study, we found that rVpr activated the TLR4/MyD88-dependent cellular cascade in human MDMs, leading to the production of IL-6. rVpr-induced IL-6 production depended on the activation of NF-κB and MAPK signaling and the phosphorylation of C/EBP-β. Moreover, we found that rVpr-induced oxidative stress caused the formation of OxPC, and pretreatment with DLH3, a mAb against OxPC, blocked rVpr-induced IL-6 production and the phosphorylation of C/EBP-β. These data indicate that IL-6 production is initiated by the formation of OxPC generated by the effects of rVpr-induced oxidative stress. Varin et al. [36] reported that a synthetic Vpr peptide activated AP-1, JNK, and NF-κB signaling, resulting in increased viral replication; however, the molecular mechanism involved remains to be clarified. Our current work provides an explanation for the activation of these cellular responses by Vpr-induced oxidative stress. We hypothesize that OxPC, as the most upstream event, extracellularly activates TLR4-mediated signaling. This notion is supported by previous data reported by Imai et al. [27] that TLR4 signaling is activated by acid challenge or treatment with H5N1 in mouse lungs via OxPC. They detected OxPC generated in bronchoalveolar lavage in affected mouse lungs and showed that its activity was blocked by a mAb against OxPC. However, our blocking experiments with DLH3 cannot exclude the possibility that the formation of OxPC and activation of TLR4-mediated cellular signals are required independently for Vpr-induced IL-6 production. Here, we showed that OxPC-triggered cellular signals were dependent on MyD88, whereas those induced by SARS-CoV were shown to be MyD88-independent [27]. These discrepant observations may have been a result of differences in the experimental conditions applied; we used human monocytes/macrophages, whereas Imai et al. [27] used rodent cells.

ROS are likely generated as a result of the mitochondrial dysfunction caused by Vpr. With regard to the mechanism of mitochondrial dysfunction, it has been shown that Vpr binds ANT, a member of the permeability transition pore complex [39], and disrupts the MMP [17]. The domain of Vpr involved in mitochondrial toxicity has been identified as the region encompassing aa 72–83, and arginine residues at positions 73, 77, and 80 (R73, R77, and R80) were defined as being critical for the interaction with ANT [39]. We showed previously that a mutant rVpr protein with alanines in place of the three arginines lacked the ability to impair the MMP and neurite outgrowth [17]. Additionally, a mutant virus carrying Vpr, altered at R77, was detected in patients who were HIV-1-positive and diagnosed as long-term nonprogressors [40], suggesting that the Vpr-induced killing activity of T cells might be linked directly to the clinical outcome of these individuals.

Our finding that exogenously added rVpr reactivated viral reproduction in latently infected cells will broaden our understanding of the pathophysiology in HIV-1-positive patients. HAART dramatically improves the prognosis of HIV-1-positive patients; unfortunately, however, it was concluded that complete eradication of the virus by the chemotherapeutics currently available would take more than 60 years [41]. Such observations underscore the importance of preventing new episodes of viral infection or restraining viral production from latent reservoirs. Vpr has been postulated to function as a necessary factor in the primary infection of resting macrophages and to enhance viral reproduction following latency. As reported previously [13], Vpr is present in the plasma of HIV-1-positive patients, and we ascertained that rVpr added exogenously at the nM level, which is comparable with the level observed in patient plasma, reproducibly reactivated viral production from latency via IL-6 production. Although autoantibodies to Vpr [42] might neutralize its activity, we suggest the importance of monitoring patient plasma Vpr levels in the context of the clinical course. Our results provide a rationale for the development of novel anti-AIDS therapeutics against Vpr.

REFERENCES

1. Palella, F. J., Delaney, K. M., Moorman, A. C., Loveless, M. O., Fuhrer, J., Satten, G. A., Aschman, D. J., Holmberg, S. D. (1998) Declining morbidity and mortality among patients with advanced human immunodeficiency virus infection. HIV Outpatient Study Investigators. *N. Engl. J. Med.* **338**, 853–860.
2. Siliciano, J. D., Kajdas, J., Finzi, D., Quinn, T. C., Chadwick, K., Margolick, J. B., Kovacs, C., Gange, S. J., Siliciano, R. F. (2003) Long-term follow-up studies confirm the stability of the latent reservoir for HIV-1 in resting CD4+ T cells. *Nat. Med.* **9**, 727–728.
3. Finzi, D., Hermankova, M., Pierson, T., Carruth, L. M., Buck, C., Chaisson, R. E., Quinn, T. C., Chadwick, K., Margolick, J., Brookmeyer, R., Gallant, J., Markowitz, M., Ho, D. D., Richman, D. D., Siliciano, R. F. (1997) Identification of a reservoir for HIV-1 in patients on highly active antiretroviral therapy. *Science* **278**, 1295–1300.
4. Folks, T. M., Justement, J., Kinter, A., Dinarello, C. A., Fauci, A. S. (1987) Cytokine-induced expression of HIV-1 in a chronically infected promonocyte cell line. *Science* **238**, 800–802.